SRNL-STI-2011-00278, Rev. 0

Keywords: tank mixing, kaolin, seed particles, pilot-scale, cohesive

Retention: *Permanent*

Demonstration of Mixing and Transferring Settling Cohesive Slurry Simulants in the AY-102 Tank

D. J. Adamson
Savannah River National Laboratory

P. A. Gauglitz
Pacific Northwest National Laboratory

July, 2011

Savannah River National Laboratory
Savannah River Nuclear Solutions
Aiken, SC 29808

Prepared for the U.S. Department of Energy under contract number DE-AC09-08SR22470.

DISCLAIMER

Printed in the United States of America

Prepared for
U.S. Department of Energy

REVIEWS AND APPROVALS

AUTHORS:

D. J. Adamson, SRNL Engineering Development Laboratory Date

P. A. Gauglitz, PNNL Date

TECHNICAL REVIEW:

J. L. Steimke, SRNL Engineering Development Laboratory Date

APPROVAL:

B. J. Giddings, Manager, SRNL Engineering Development Laboratory Date

S. L. Marra, Manager, SRNL E&CPT Research Programs Date

M. G. Thien, WRPS Task Lead Date

EXECUTIVE SUMMARY

In support of Hanford's waste certification and delivery of tank waste to the Waste Treatment and Immobilization Plant (WTP), Savannah River National Laboratory (SRNL) was tasked by the *Washington River Protection Solutions* (WRPS) to evaluate the effectiveness of mixing and transferring tank waste in a Double Shell Tank (DST) to the WTP Receipt Tank. The work discussed in this report (Phase III) addresses the impacts cohesive simulants have on mixing and batch transfer performance. This work is follow-on to the previous tasks "Demonstration of Mixer Jet Pump Rotational Sensitivity on Mixing and Transfers of the AY-102 Tank" [1] and "Demonstration of Simulated Waste Transfers from Tank AY-102 to the Hanford Waste Treatment Facility" [2]. The cohesive simulants for Phase III were investigated and selected jointly by SRNL and PNNL and a white paper was written on this evaluation [3]. The Phase III testing and demonstrations of cohesive simulants was a joint effort performed as collaboration between SRNL and PNNL staff.

The objective of the demonstrations performed in Phase III was to determine the impact that cohesive particle interactions in the simulants have on tank mixing using $1/22^{nd}$ scale mixing system and batch transfer of seed particles. This testing is intended to provide supporting evidence to the assumption that Hanford Small Scale Mixing Demonstration (SSMD) testing in water is conservative.

The batch transfers were made by pumping the simulants from the Mixing Demonstration Tank (MDT) to six Receipt Tanks (RTs), and the consistency in the amount of seed particles in each batch was compared. Tests were conducted with non-Newtonian cohesive simulants with Bingham yield stress ranging from 0.3 Pa to 7 Pa. Kaolin clay and 100 μm stainless steel seed particles were used for all the non-Newtonian simulants. To specifically determine the role of the yield stress on mixing and batch transfer, tests were conducted with a Newtonian mixture of glycerol and water with at viscosity of 6.2 cP that was selected to match the Bingham consistency (high shear rate viscosity) of the higher yield stress kaolin slurries. The water/glycerol mixtures used the same 100 μm stainless steel seed particles.

For the transfer demonstrations in Phase III, the mixer jet pumps were operated either at 10.0 gpm (28 ft/s nozzle velocity, U_oD=0.63 ft^2/s) or 8.0 gpm (22.4 ft/s nozzle velocity, U_oD=0.504 ft^2/s). All batch transfers from the MDT to the RTs were made at 0.58 gpm (MDT suction velocity 3.95 ft/s).

The demonstrations that used simulants that ranged from 1.6 Pa to 7 Pa yield stress had the most successful batch transfer of solids to the RTs in terms of the total quantity of seed particles transferred. Testing suggest that when mixing water/seed particles and transferring, water provides the least desired batch transfer of solids based on the total quantity transferred. For the water tests, large dead zones of solids formed in the MDT and fewer solids get transferred to the RTs. For simulants with a yield stress of 0.3 Pa and below, the batch transfer behavior in terms of total transfer of seed particles was slightly higher than water test results. The testing did show somewhat more batch-to-batch variation in the transfer of seed particles with the slurries in comparison to water. A comparison of batch transfers with the kaolin slurries that had Bingham consistencies (viscosities) that were

nearly the same as the Newtonian glycerol/water mixtures showed that the kaolin slurries with Bingham yield stresses of 1.6 and 7 Pa gave better batch transfer of seed particles based on the total quantities transferred. Overall, the batch transfer testing results show that testing with water is conservative, since using a simulant with a yield stress and/or elevated viscosity always resulted in a better total transfer of solids.

TABLE OF CONTENTS

LIST OF FIGURES

LIST OF TABLES

LIST OF ABBREVIATIONS

cP	Centipoise
DST	Double shell tank
EDL	Engineering Development Laboratory
gpm	Gallons per minute
ID	Inner diameter
MDT	Mixing Demonstration Tank
MJP	Mixing Jet Pumps
OD	Outer diameter
PNNL	Pacific Northwest National Laboratory
PSD	Particle size distribution
PVC	Polyvinyl Chloride
rpm	Revolutions per minute
RT	Receipt Tank
SRNL	Savannah River National Laboratory
SS	Stainless steel
SSMD	Small Scale Mixing Demonstration (Hanford)
TSPP	tetrasodium pyrophosphate
TTQAP	Task Technical and Quality Assurance Plan
TTR	Task Technical Request
WRPS	*Washington River Protection Solutions*
WTP	Waste Treatment Plant
Y_G	Gravity yield parameter
Re_τ	Yield Reynolds number
RMS	Root means square
YS	Yield Stress

1.0 INTRODUCTION

The Hanford double shell tank (DST) system provides the staging location for feeding tank waste to the Waste Treatment and Immobilization Plant (WTP). ICD-*19 "Interface Control Document for Waste Feed Delivery*" (24590-WTP-ICD-MG-01-019) [4] includes a WTP acceptance criterion that describes physical and chemical characteristics of the waste that must be certified as acceptable prior to waste transfer from the DSTs to the WTP. The baseline feed delivery concept includes equipment capable of mixing the DST waste, obtaining representative samples of the DST contents, and delivering waste to the WTP within acceptable tolerance bands of waste chemical and physical properties. Understanding the three dimensional performance of the DST mixing systems is necessary to define the specific functional requirements of the DST sampling and feed transfer systems. The early stages of the Waste Feed Delivery Demonstration Program are focused on demonstrating, in a scaled environment, the performance of mixing the contents in a DST tank and transferring the contents out of the tank. The Phase III testing and demonstrations of cohesive simulants was jointly performed in a collaboration between SRNL and PNNL staff.

During the previous work reported in "Demonstration of Mixer Jet Pump Rotational Sensitivity on Mixing and Transfers of the AY-102 Tank" and "Demonstration of Simulated Waste Transfers From Tank AY-102 to the Hanford Waste Treatment Facility", it was determined that the jet velocity of the Mixer Jet Pumps (MJPs) had the biggest impact on mixing and batch transfer of solids from the 1/22nd scale MDT. The mixing/transfer demonstrations from this previous work showed that there was good consistency (equal amount in each batch) of solids transferred between batches no matter what test parameter was changed and increasing the jet velocity increased total amount of solids transferred.

This report focuses on the impact that cohesive particle interactions in simulants, which cause the simulants to be non-Newtonian and have a yield stress, may have on batch transfers from the 1/22nd scale MDT to six individual Receipt Tanks. As with the demonstrations of Phase II testing, these demonstrations modeled the batch transfers from the AY-102 Tank to the WTP receipt tank where HLW slurry will be delivered in 160,000 gallon batches.

Previous Small Scale Mixing Demonstration (SSMD) mixing and batch transfer studies focused on quantifying the mixing and batch transfer behavior of non-cohesive particles in a Newtonian liquid such as water.[5] In a recent study as part of the overall SSMD project, Gauglitz et al. (2010) [6] evaluated the potential role of cohesive particle interactions, such as in a Bingham plastic, on mixing and transfer behavior. This study noted that there are no existing studies or data that specifically quantify the role of cohesive interactions on the uniformity of the waste during mixing and transfers, and concluded that cohesive particle interaction will have multiple effects on uniformity through a number of different mechanisms. Some of the effects improve solids uniformity, while others will likely degrade uniformity. The overall recommendation by Gauglitz et al. (2010) [6] was to conduct scoping tests to determine the magnitude of the impact caused by cohesive particle interactions on mixing. The purpose of this study is to quantify the impact of cohesive particle interactions

on mixing and batch transfer behavior with simulants that span the expected range of behavior of actual tank waste.

Gauglitz et al. (2010) [6] discussed how cohesive particle interaction typically causes a slurry to have non-Newtonian rheology and exhibit a yield stress, such as in a Bingham plastic. Typically, the yield stress increases as the magnitude of the cohesive interactions is increased by changing the particle characteristics or by increasing the particle concentration. Gauglitz et al. (2010) also summarized available yield stress data for Hanford waste and a yield stress range of 0–10 Pa encompasses the majority of DST waste if the solids in the DSTs are uniformly suspended. If additional solids are added to the DSTs or if the waste is diluted, this yields stress range may change, but until these changes are known a reasonable assumption for testing is to consider the full yields stress range of 0-10 Pa.

Adamson et al.[3] summarize the preliminary laboratory evaluation and selection of the cohesive simulants for Phase III testing. Kaolin slurries with a range of concentrations to vary the yield stress along with 100 μm stainless steel seed particles were selected for all the non-Newtonian simulants. To specifically determine the role of the yield stress due to cohesive particle interactions on mixing and batch transfers, a glycerol/water mixture with 100 μm stainless steel particles was tested. The mixture was selected to have a viscosity that matches the Bingham consistency (high shear rate viscosity) of the higher yield stress kaolin slurries.

2.0 EXPERIMENTAL METHOD

2.1 Overview

The test system used for the mixing and batch transfer demonstrations is shown in Figure 1. This is the same test system used in Phase II Testing. For this Phase III testing the rotational synchronization of the MJP was not controlled. The Transparent 1/22nd MDT has an ID of 40.5" and a height of 30" with a transparent bottom for visual observations from the underside. The geometrically scaled obstructions consisted of 22 air lift circulators (ALC), heating coil, a transfer pump feed line and two Mixer Jet Pumps (MJPs). The geometrically scaled obstructions simulated the obstructions found in the full-scale AY-102 Tank. The obstructions were installed in the MDT for all Phase III testing and demonstrations.

As with all past testing, there was only one slurry pump (Pump 1) that fed both the MJPs. The slurry pump was located external to the MDT and the flow rate was controlled by a variable speed drive. The test fluid (simulant) was pumped from the MDT through the inlet at the very bottom of the MJPs to the slurry pump and then circulated back to the MJP down to the jet nozzles. The simulant in the MDT mixed when the fluid flowed out of the two nozzles on each MJP. Detail drawings of the MJP and the obstructions are given in Appendix A.

The batch transfers were made with a progressive cavity pump (Pump 3), the same transfer pump used in Phase II (Moyno Pump, Model 33201). A progressive cavity pump was chosen for its resilience to solids induced wear and its stability of operation in the flow regime required. All batch transfers out of the MDT made for Phase III were made at 0.58 gpm. With a $^{3}/_{8}$", 0.065" wall stainless steel tubing at the transfer suction point in the MDT, the suction velocity was 3.95 ft/sec. Flexible 3/8" tubing was used from the suction line at the MDT to the transfer pump and a ¼", 0.035" wall stainless steel tubing was used from Pump 3 to the Receipt Tanks. The transfer line was reduced to a ¼" tube due to concerns of low velocity solids falling out in the line, thus plugging the transfer line. With a ¼", 0.035" wall tube the velocity increased to 7.3 ft/sec.

No modifications were made to the demonstration system from Phase II. However the slurry pumps, MJPs, and transfer pump were rebuilt due to pump wear.

Table 1 provides important parameters associated with the AY-102 Tank and the 1/22nd scale MDT and transfer systems.

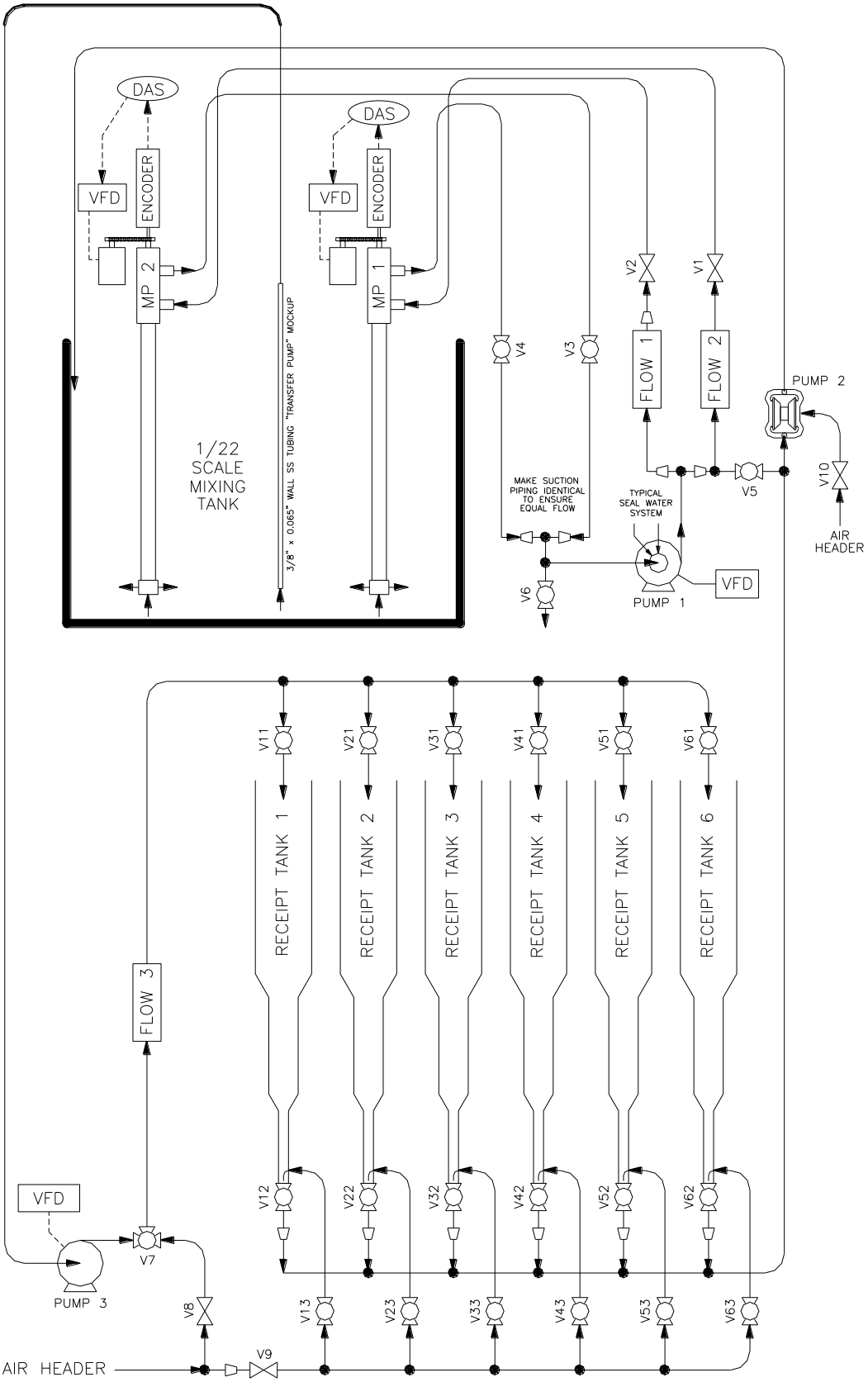

Figure 1: Drawing of the Mixing/Transfer Demonstration System

Table 1: Full Size and Scaled Parameters, Phase III

Parameter Description AY-102	Full Scale	Model@ $^1/_{22}$=0.045 scale factor
Tank diameter	75 ft (900 inches)	40.5 inches
Tank operating height	364 inches	16.5 inches
Total waste height	347 inches	15.6 inches
Sludge height	55 inches	-
Supernate height	292 inches	-
Total waste volume	955,085 gal	87 gallons
Batch volume to WTP	160,000 gal	14.3 gal
Residence mixing time AY-102	45.2 minutes	
Flow for scaled model to have full scale residence mixing time	-	0.47 gal/min/nozzle
Nozzle velocity at full-scale residence	-	2.6 ft/sec
Pump location from tank center	22 ft	11.9 inches
Pump above tank bottom	6 inches	0.27 inches
Nozzle diameter	6 inches	0.27 inches
Nozzle location from bottom of pump	9 inches	0.41 inches
Pump rotational speed	0.2 rpm	1.6 rpm
Pump flowrate Nozzle Exit Velocity	5280 gal/min/nozzle 60 ft/sec	10.8 gal/min/nozzle 60 ft/sec
1/22nd MJP flowrate (8 gpm) [(a)] Nozzle Exit Velocity	-	4 gal/min/nozzle 22.4 ft/sec/nozzle
U_oD at a flowrate of 8 gpm MJP	-	0.504 ft^2/s
Pump flowrate (power cal.) [(b)]	5280 gal/min/nozzle	5.0 gal/min/nozzle
Nozzle velocity (power calculation) [(b)]	60 ft/sec	28 ft/sec/nozzle
U_oD (power cal.), 10 gpm MJP	-	0.63 ft^2/s
Liquid density	1,150 kg/m^3	1,000 kg/m^3 (water)
Solids density	2,500 kg/m^3	Kaolin: 2,650 kg/m^3 SS: 8,000 kg/m^3
Viscosity of liquid	2.8 cP	1 to 9.1 cP (See simulants)
Air mixers (22 in tank)	30 inches	1.35" (used 1.25")
Air mixers above tank bottom	30 inches	1.35 inches
Heating coil dia (1 in tank)	40.375 inches	1.8 " (used 1.75")
Transfer pump outlet diameter	12 inches	-
Transfer pump inlet diameter	2.25 inches	0.1" (used 3/8" 0.065 wall SS tube)
Transfer pump above tank bottom	5 inches	0.23 inches (used ¼")
Transfer pump, pump rate	90 – 140 gpm	Used 0.58 gpm
Transfer pump suction, velocity	7.3 ft/s, 11.3 ft/s	Used 3.95 ft/s
Particle size distribution	2.5 ~ 16.8 μm	Kaolin - No PSD SS - -106/ +75 μm

(a) For constant power per unit volume in a geometrically scaled tank, the jet velocity at the pilot scale is related to the full scale velocity and the scale factor by $U_{j\text{-}pilot} / U_{j\text{-}full} = (1/SF)^{1/3}$. This relationship is discussed later in this section. For the pilot tank, $U_{j\text{-}pilot} = (60 \text{ ft/s}) (1/22)^{1/3} = 21.4$ ft/s and a MJP flow of 8 gpm essentially matches this velocity.

(b) An alternate approach for selecting a jet velocity for small-scale testing is to assume the power, P, per unit volume, V, is not constant, but changes with scale. Based on a literature value, Adamson et al., [5] (see appendix C) used $(P/V)_{pilot} / (P/V)_{full\ scale} = SF^{1/4}$ which results in $U_{j\text{-}pilot} / U_{j\text{-}full} = (1/SF)^{1/4}$ for a geometrically scaled tank. For the pilot tank, $U_{j\text{-}pilot} = (60 \text{ ft/s})(1/22)^{1/4} = 27.7$ ft/s and a MJP flow of 10 gpm essentially matches this velocity.

Three flow meters were used in the transfer demonstrations to measure the flow rate of simulant being sent to the MJPs and the batch transfers. Table 2 provides an instrument list along with calibration information of the instruments.

Table 2: Instrument List

M&TE #	Description	Calibration range	Uncertainty
TR-03811	Magnetic flow meter, ABB Instrumentation Inc.	0 – 25 gpm	± 0.22 gpm
TR-03674	Magnetic flow meter, ABB Instrumentation Inc.	0 – 25 gpm	± 0.18 gpm
TR-03680	Magnetic flow meter, Fischer Porter for Transfers	0 – 1.6 gpm	± 0.009 gpm

The demonstration system was designed such that six independent batch transfers could be made from the MDT. This simulates the multiple 160,000 gallon batches that will be transferred to the WTP receipt tank from the AY-102 Feed Tank. Figure 1 shows valve configurations to control the batch transfers from the MDT to the six Receipt Tanks.

The same six (6) Receipt Tanks that were used in Phase II testing were also used in Phase III testing. The tanks are transparent (clear PVC) on the lower section of the tank (except for reducers) to allow for measuring the volume of solids that were transferred in each batch. As shown in Figure 2, the bottom section of the tank makes a smooth transfer from a 6", schedule 40 pipe (between point 3 and point 4) to a 3", schedule 40 transparent PVC pipe (between point 1 and point 2).

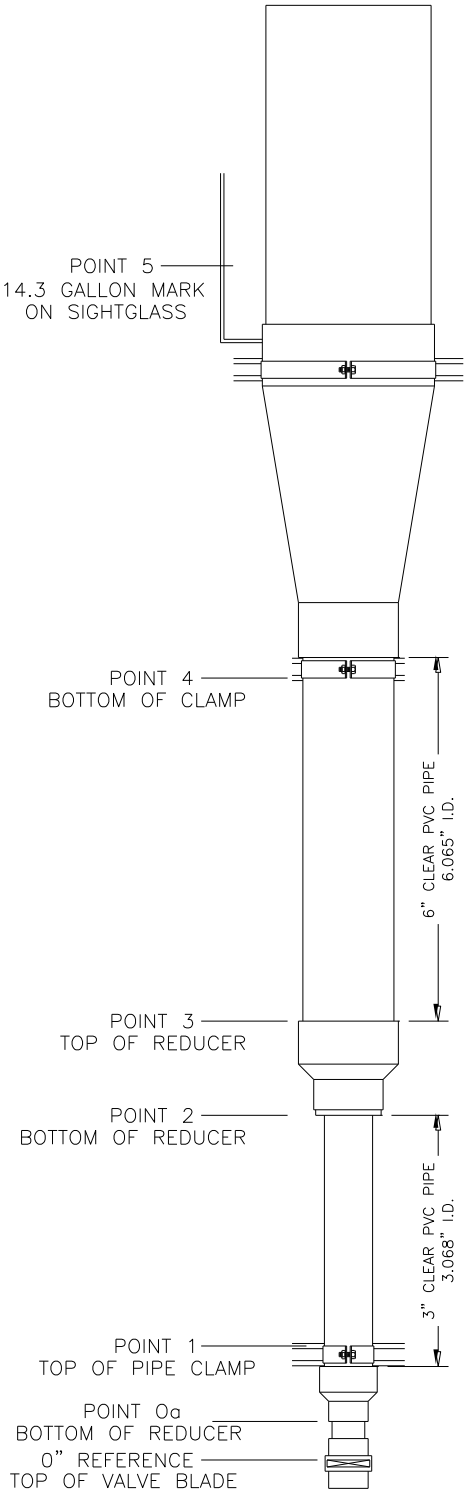

Figure 2: Receipt Tank Drawing

The Receipt Tanks hold approximately 22 gallons. Each tank was calibrated at six different elevations. Point 5 on the sight glass depicts the maximum volume (14.3 gallons) that was

transferred in each batch. Table 3 gives the calibration data of each of the six Receipt Tanks.

Table 3: Receipt Tank Calibrations

	RT-1		RT-2		RT-3		RT-4		RT-5		RT-6	
Point	inch	gallon	inch	gallon	inch	gallon	inch	gallon	inch	gallon	inch	gallon
0a	2.94	0.038	2.94	0.038	3.0	0.039	2.94	0.038	3.0	0.038	2.94	0.038
1	8.38	0.26	8.38	0.19	8.32	0.20	8.56	0.19	8.75	0.20	8.69	0.21
2	23.06	0.74	23.06	0.65	23.06	0.66	23.06	0.65	23.13	0.66	23.13	0.66
3	30.00	1.32	30.00	1.23	30.06	1.22	30.13	1.23	29.94	1.23	30.00	1.26
4	55.00	4.40	55.00	4.30	55.00	4.30	55.00	4.31	54.75	4.29	54.63	4.32
5	-	14.30	-	14.30	-	14.30	-	14.30	-	14.30	-	14.30

Air spargers were designed into the bottom of each of the Receipt Tanks. The spargers were used to mix 600 ppm tetra-sodium pyrophosphate (TSPP) into the simulant and to mix the contents of the receipt tanks before pump out. The addition of TSPP was used to reduce the yield stress of the kaolin slurries and allow the SS seed particle to settle into a layer at the bottom of each receipt tank. To add the TSPP, 1 liter of a concentrated solution TSPP was pumped to the bottom (in the location of the sparger) of the each RT in about 3 minutes. This allowed the TSPP to mix better/quicker with the simulant. The spargers worked well to mix in the TSPP and kaolin together.

As with Phase II, the operating liquid level in the scaled MDT was scaled from the total liquid level (347") currently in the AY-102. The mixing demonstration used approximately 15.6" of simulant to be geometrically scaled with the Hanford tanks. At the end of the 6th batch transfer there was approximately 1.5 gallons (1" in the MDT equals 5.58 gallons) or more of simulant left in the MDT. The transfer suction line was placed ¼" off the bottom the MDT.

For scaled testing with rotating jets, the rotation rate in different size tanks can be scaled to give equal jet behavior, though there is more than one selection of characteristic time scales for scaling the rotation rate (Bamberger et al. 1990, Enderlin et al. 2003). Bamberger et al. (1990) showed that kinematic similarity of the jet can be maintained by comparing the time scale for the jet to rotate around the tank to the time it takes fluid moving at the jet velocity to travel a characteristic distance such as the tank diameter. Both Bamberger et al. (1990) and Enderlin et al. (2003) consider alternate time scales. For the kinematic relationship, the two time scales are given as follows:

$$\text{Jet time scale} = D / U_j$$
$$\text{Rotation rate time scale} = 1/\omega$$

where, D = tank diameter, U_j = jet velocity, and ω = jet rotation rate. Keeping the ratio of these time scales the same at both pilot and full scale gives the following result.

$$D_{pilot}\ \omega_{pilot} / U_{j\text{-}pilot} = D_{full}\ \omega_{full} / U_{j\text{-}full}$$

Rearranging and using the scale factor definition of $SF = D_{full} / D_{pilot}$ gives

$$\omega_{pilot} = \omega_{full} (D_{full} / D_{pilot})(U_{j\text{-}pilot} / U_{j\text{-}full}) = \omega_{full} (SF) (U_{j\text{-}pilot} / U_{j\text{-}full})$$

There are a number of alternative approaches for the determining the appropriate ratio of jet velocities in the different scale tanks. One approach for scaled testing is to maintain an equal power per volume in the different tanks (Paul et al. 2004). The tank volume is calculated by:

$$\text{Tank Fluid Volume} = (\pi/4) D^2 H$$

The hydraulic power from each jet is given by, Bamberger et al. 2005):

$$\text{Power (each jet)} = (\pi/8) U_j^3 d_j^2$$

where d_j is the jet diameter. Keeping the ratio of power to fluid volume the same in both the pilot and full scale tanks, and assuming geometric scaling so the ratio of jet diameters and tank diameters are equal, gives the following relationship for the ratio of jet velocities at constant power per volume:

$$U_{j\text{-}pilot} / U_{j\text{-}full} = (1/SF)^{1/3}$$

Combining this jet velocity relationship with the rotation rate equation above gives the following result for the scaled rotation rated in the pilot-scale tank.

$$\omega_{pilot} = \omega_{full} (SF)^{1\text{-}1/3}$$

For the full-scale rotation rate and scale factor in Table 1, the rotation rate in the pilot-scale tank is given as follows:

$$\omega_{full} = 0.2 \text{ rpm}$$
$$SF = 22$$

$$\omega_{pilot} = (0.2 \text{ rpm}) 22^{1 - 1/3} = 1.6 \text{ rpm}$$

This rotation rate gives kinematic similarity of the rotating jet when the jet velocity is scaled to give equal power per volume. To minimize the number of parameters changed during testing at different jet velocities, the rotation rate in all tests was held constant at 1.6 rpm.

Figure 3 is a top view picture of the MDT showing the two drive assemblies (gears and chain inside the safety guard) used to rotating the MJPs.

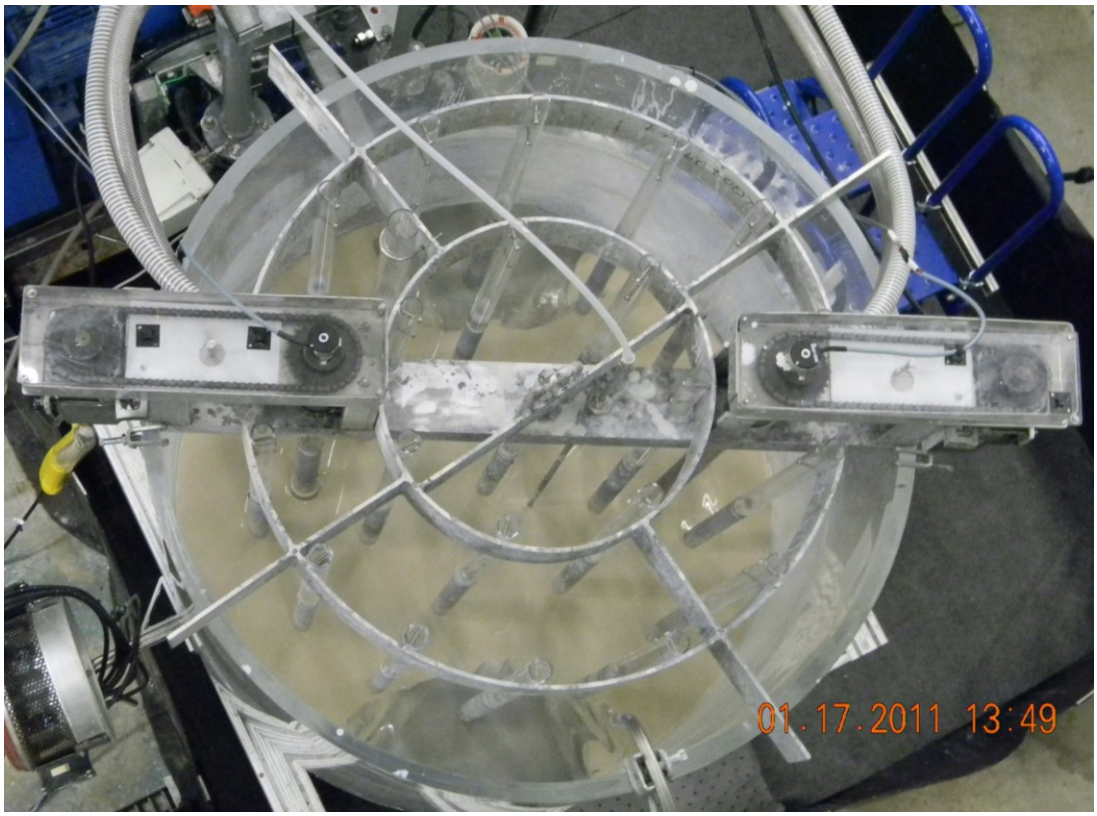

Figure 3: Drive Assemblies for MJP Rotation, End of Test 2

The rotational system worked well had no mechanical problem for all of Phase III testing.

Testing was conducted per an approved R&D Direction. Test results were also recorded in Laboratory Notebook, SRNL-NB-2010-00095.

Simulant

The recipe below for each simulant is for an 87 gallon batch except for the 19 wt% kaolin. The 19 wt% kaolin for Tests 8 and 9 was mixed in one large batch without the SS, which was added for each test. For Test 8 and 9 the target was to have 1.5 Pa ± 0.5 Pa Bingham yield stress kaolin for both tests. The stainless steel was the same mass in all batch recipes, equating to 5 wt% in water.

Stainless steel particles (PSD -106/+75 μm) were used as seed particles in all tests that were conducted during Phase III. The PSD used here is from the vendor, meaning the SS particles are between 75 μm and 106 μm. The advantage of using stainless steel is the SS particles are very dense, making them difficult to suspend in the suspending fluid. Because these particles are not easily suspended under the planned test conditions, they are suitable for observing changes in mixing behavior with the different simulants. The SS particles can be seen visually in the kaolin during mixing allowing their suspension off the bottom of the MDT to be observed visually, and their dark color during the batch transfers contrasts well

with the kaolin to allow visual comparisons of the amount of SS in each of the six batches transferred.

Water and 5 wt% Stainless Steel (SS)
Water: 312.86 Kg (689.74 lbs)
SS: 17.29 Kg (38.1 lbs)

14 wt% Kaolin and SS
Kaolin: 46.1 Kg (101.65 lbs)
Water: 283.2 Kg (624.4 lbs)
SS: 17.29 Kg (38.1 lbs)

19 wt% Kaolin (two batches, for Tests 8 and 9 with settled SS bed)
Kaolin: 136.67 Kg (301.31 lbs)
Water: 596.93 Kg (1,316.0 lbs)

For Test 8 and Test 9 a bed of settled solid, with the total mass of added SS (23.29 Kg) was laid in the bottom of the MDT. The SS was mixed in with a volume of the kaolin slurry, resulting in about 1" of settled solids in the MDT. The kaolin slurry was then gently pumped into the MDT taking care not to disturb the bed of solids.

23.4 wt% Kaolin and SS
Kaolin: 87.81 Kg (193.6 lbs)
Water: 288.21 Kg (635.4 lbs)
SS: 17.29 Kg (38.1 lbs)

52 wt% Glycerol and SS (6.2 cP at 70˚ F)
Glycerol: 194.23 Kg (428.2 lbs)
Water: 178.58 Kg (393.7 lbs)
SS: 17.29 Kg (38.1 lbs)

Solids densities:
Stainless Steel (SS) - 8,000 kg/m^3, -106/+75 μm (vendor's PSD)
Kaolin – 2,650 kg/m^3

Tetra-sodium Pyrophosphate ($Na_4P_2O_7$**)**
A dispersant, tetra-sodium pyrophosphate was used to disperse the kaolin particles. Adding TSPP eliminated the yield stress of the slurry for sufficiently high concentrations, and 600 ppm had been determined previously to be sufficient for this purpose.[3] As mentioned previously, adding TSPP allowed the SS to settle from the kaolin slurry in the receipt vessel. TSPP also increased pH. Kaolin slurries with wt% of 14 wt% or higher exhibit yield stress making the slurry non-Newtonian, but only the 19 wt% and 23.4 wt% slurries needed TSPP addition in the receipt tanks. TSPP was added only to the non-Newtonian batch transfers in the receipt tanks.

Test Matrix

Table 4 is the test matrix for Phase III demonstrations. For Phase III, all batch transfers were continuous at 0.58 gpm, resulting in a suction velocity of 3.95 ft/s. The continuous transfer is conducted by continuously operating the mixer pumps and slurry transfer pump and not allowing the tank contents to settle between batches. Once a batch of 14.3 gallons was transferred to a Receipt Tank, the valve line up was changed, sending the subsequent batch to the next Receipt Tank. While this batch transfer process does not match expected WTP feed logistics, it was demonstrated in previous testing that it does not impact the batch transfer consistency. [2] The continuous batch transfers were also used during Phase II.

Only Test 5A had TSPP while mixing in the MDT and transferring to the receipt tanks. At the end of Test 5, TSPP was added in the RTs as described previously, and the simulant was pumped back to the MDT to conduct Test 5A. Test 5A was conducted to compare the mixing and batch transfer results for the exact simulant used in Test 5, but with the cohesive particle interactions eliminated by the addition of 600 ppm.

Table 4: Test Matrix for Cohesive Simulant Demonstrations, Phase III

Test #	Simulant	Batch Transfer (gpm)	Transfer Type	Mixer Jet Pumps		
				Rotation (rpm)	Flowrate (gpm)	Velocity (ft/sec)
1	Water with 5 wt% SS seeds**	0.58	Continuous	1.6	10.0	28.0
2	14 wt% Kaolin 5 wt% SS seeds	0.58	Continuous	1.6	8.0	22.4
3	14 wt% Kaolin 5 wt% SS seeds	0.58	Continuous	1.6	10.0	28.0
4	23.4 wt% Kaolin 5 wt% SS seeds	0.58	Continuous	1.6	8.0	22.4
5	23.4 wt% Kaolin 5 wt% SS seeds	0.58	Continuous	1.6	10.0	28.0
5A	23.4 wt% Kaolin 5 wt% SS seeds + TSPP	0.58	Continuous	1.6	10.0	28.0
6	52 wt% Glycerol 5 wt% SS seeds	0.58	Continuous	1.6	8.0	22.4
7	52 wt% Glycerol 5 wt% SS seeds	0.58	Continuous	1.6	10.0	28.0
8 *	19 wt% Kaolin 5 wt% SS seeds	0.58	Continuous	1.6	8.0	22.4
9 *	19 wt% Kaolin 5 wt% SS seeds	0.58	Continuous	1.6	10.0	28.0

** All tests had same mass of SS particles as 5 wt% in water

* Pre-layered bed of 5 wt% SS (38.1 lbs of SS in a thin layer of 1.5 Pa kaolin) in the MDT

As previously stated, the flow rate of the batch transfers from the MDT to the Receipt Tanks was conducted at 0.58 gpm. As with Phase II, the flow rate of the transfer pump was found to be very consistent and accurate. This was determined by the flow meter and by timing the transfers and measuring the total volume.

3.0 RESULTS AND DISCUSSION

The nine transfer demonstrations were conducted in the pilot-scale system described in Section 2 and shown in Figure 4. The picture shows the 1/22nd scaled MDT on the left and the six Receipt Tanks to the right.

Figure 4: Picture of the Mixing/Transfer Demonstration System

The nine transfer demonstrations of Phase III were conducted using different simulants. Each test consisted of six batch transfers that were pumped to individual Receipt Tanks. The contents of the MDT were mixed for approximately 30 minutes with the MJPs at the specific test condition before the making the first batch transfer. With a total volume of 87 gallons in the 1/22nd MDT and each MJP operating at 8.0 gpm the residence time of the system was 5.5 minutes, allowing five tank volumes of slurry to flow through the mixer pumps during this 30-min period. This is in contrast with the residence time of the AY-102 Tank which is approximately 45 minutes (with 1,000,000 gallons). The residence time of the 1/22nd scale was one of the scaling concerns from the full scale AY-102 Tank.

Rheological analyses of the simulants were performed at SRNL. Figure 5 is a rheogram for the 0.3 Pa and 3.4 cP simulant for Test 2. This is a typical rheogram for the non-Newtonian Bingham plastic slurries of kaolin. In the rheogram, the 0.3 Pa Bingham yield stress was

determined by the-zero-shear rate intercept of a fit to the shear stress data on the ramp-up of shear rate.

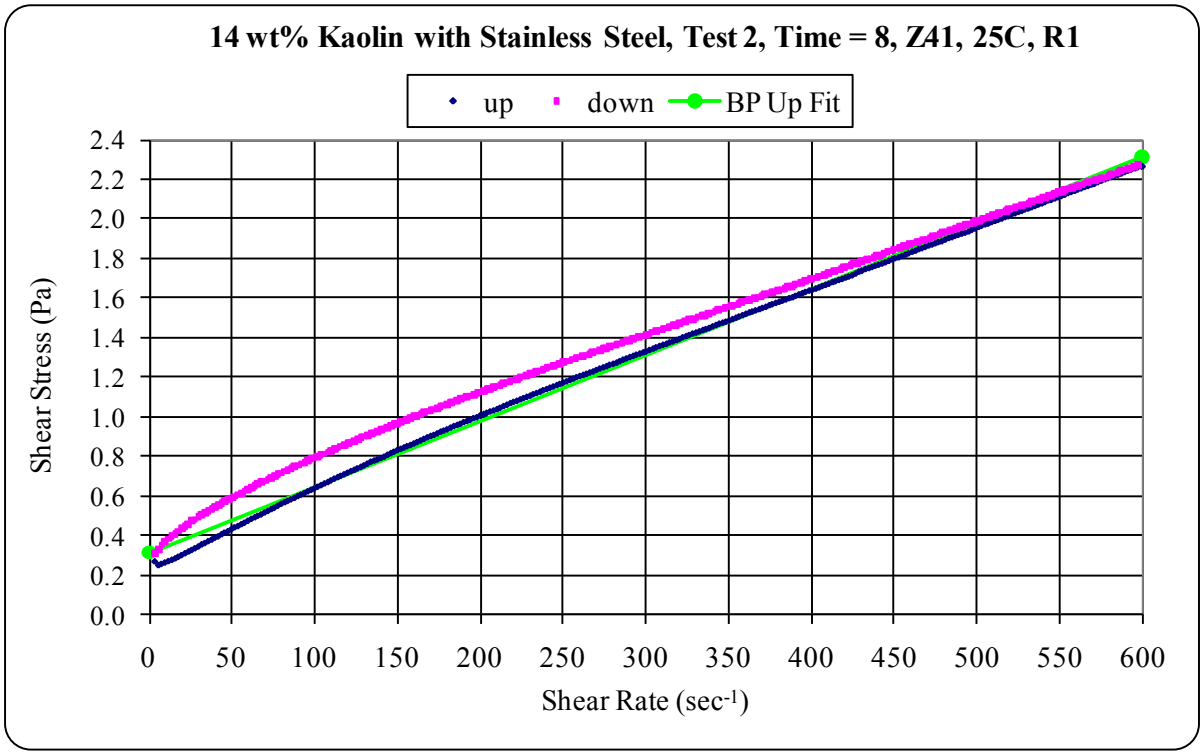

Figure 5: Rheogram of Non-Newtonian Kaolin Slurry, Test 2

Table 5 lists the rheology results of the simulants tested during Phase III. The non-Newtonian simulants tested had yield stresses that ranged from 0.3 Pa to 7.0 Pa.

Table 5: Rheology Results for Phase III Simulants

	Simulant	Bingham Yield Stress, Pa	Viscosity/Bingham Viscosity, cP
Test 1	Water + 5 wt% SS**	0	1
Test 2	14 wt% Kaolin + 5 wt% SS, (8 hr)	0.3	3.4
Test 3	14 wt% Kaolin + 5 wt% SS	0.3	3.4
Test 4	23.4 wt% Kaolin + 5 wt% SS, (4 hr)	7.0	9.1
Test 5	23.4 wt% Kaolin + 5 wt% SS, (15 min)	6.4	8.3
*** Test 5A**	23.4 wt% Kaolin + 5 wt% SS + TSPP	0	1.9
Test 6	52 wt% Glycerol + 5 wt% SS	0	6.2 @ 70˚ F
Test 7	52 wt% Glycerol + 5 wt% SS	0	6.2 @ 70˚ F
Test 8	19 wt% Kaolin, 5 wt% SS settled bed, (8 hr)	1.6	4.2
Test 9	19 wt% Kaolin, 5 wt% SS settled bed, (12+ hr)	1.9	4.5

* Same as Test 5 except for 600 ppm TSPP added to batch
** Mass of SS same for all tests as 5 wt% in water, 38.1 lbs

Figure 6 shows the viscosities from the Bingham model parameters for various simulant tested to compare the different materials. Note that 52 wt% glycerol/water mixture has a viscosity that is closest to the high shear rate viscosity of the 19 wt% and 23.4 wt% kaolin slurries. The 23.4 wt% kaolin with 600 ppm TSPP has a constant viscosity that is slightly higher the water, but well below the high shear rate viscosity of the 23.4 wt% slurry without TSPP.

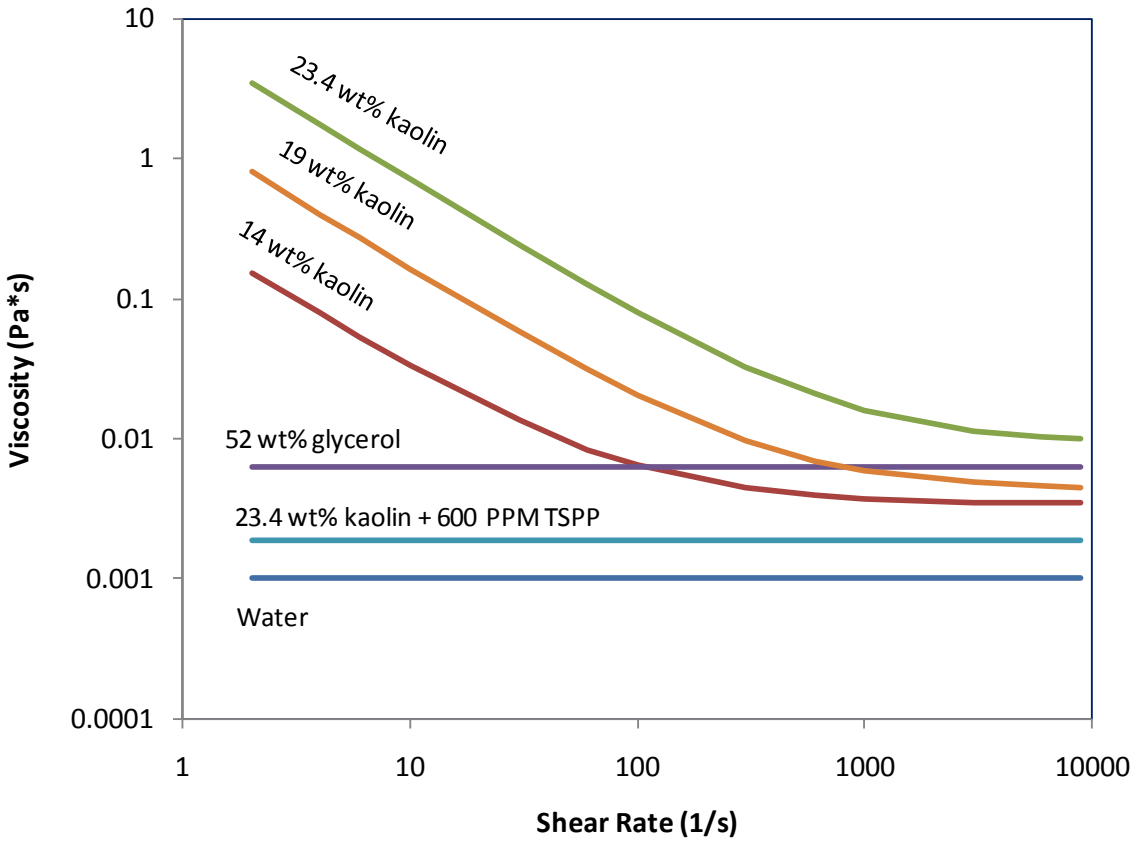

Figure 6: Comparison of Simulant Rheology

Cleaning Radius Results for Non-Rotating Jet

Cleaning radius tests were conducted with both rotating and non-rotating mixer jet pumps. The results for the non-rotating tests will be discussed here and the results with rotating jets will be discussed later in this section. The cleaning radius of the jet was investigated by viewing the operation of the MJPs through the transparent bottom of the MDT as shown in Figure 7 and noting the farthest distance where the bottom of the vessel was cleared by the jet. The cleaning radius was recorded as a function of time, but the steady state distance after a few minutes of clearing was the primary measurement. In Figure 7, the simulant was 14 wt% kaolin /5 wt% SS. The jet was directed toward the dead zone (the location where the tank wall was farthest away from the jet) which was identified by a stick-on tape measure for taking length measurements. In Figure 7, the white area is the flow field from the MJP's two jet nozzles where the jets have displaced settled SS seed particles, in this case to a distance of just over 17 in. The dark area is the fast settling stainless steel particles. In low yield stress simulants such as this 0.3 Pa kaolin slurry, the stainless steel particles were settling out of the kaolin slurry.

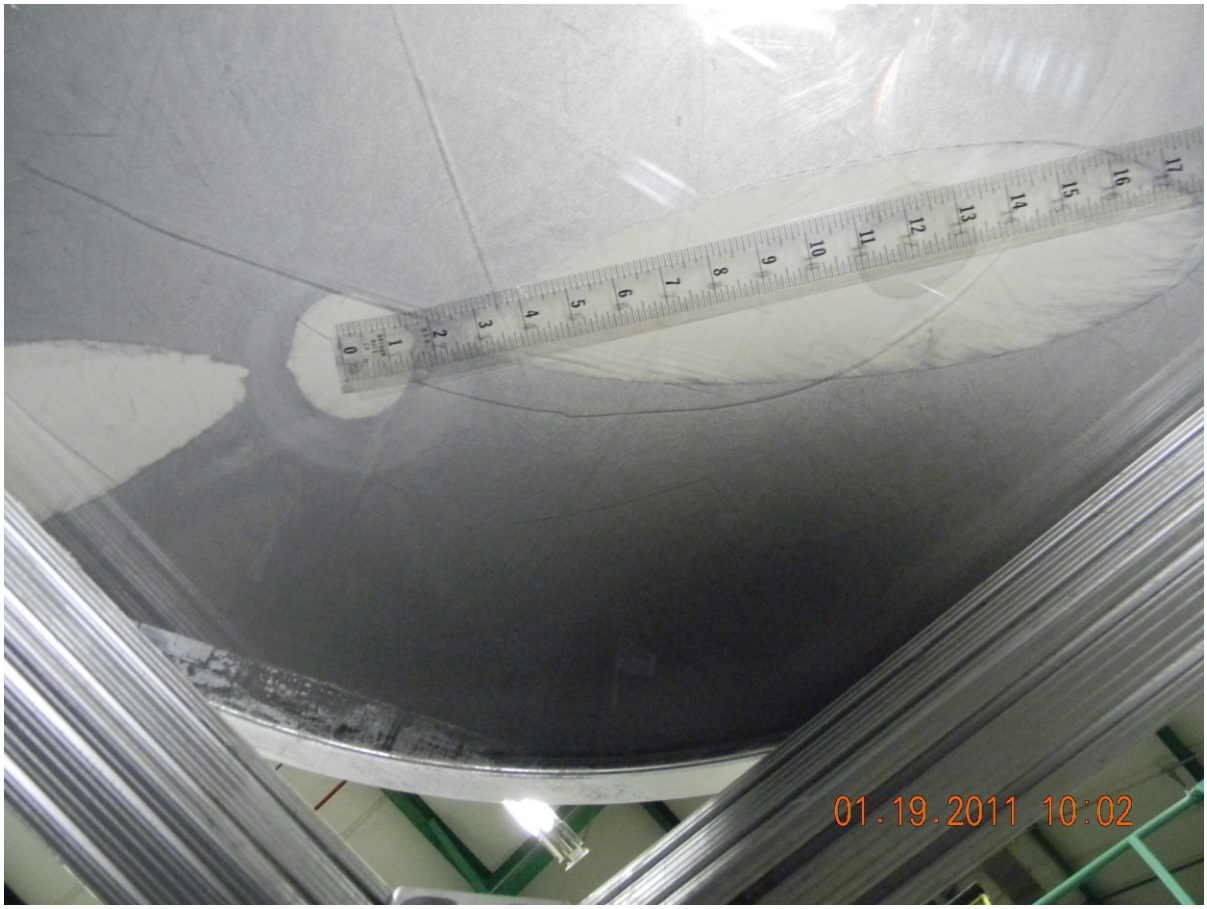

Figure 7: MJP Jet Mixing, Under MDT View, 0.3 Pa Simulant, Test 3

In the high yield stress simulants such as the 7.0 Pa simulant used in Test 4, very few of the SS particles settled out of the kaolin slurry during the non-rotating jet cleaning radius test as shown in Figure 8, although the farthest distance the jet would displace the SS seed particles was easily seen. Comparing Figures 7 and 8, one can see that there are few black particles settling from the 7.0 Pa simulant when compared to the 0.3 Pa simulant of Figure 7.

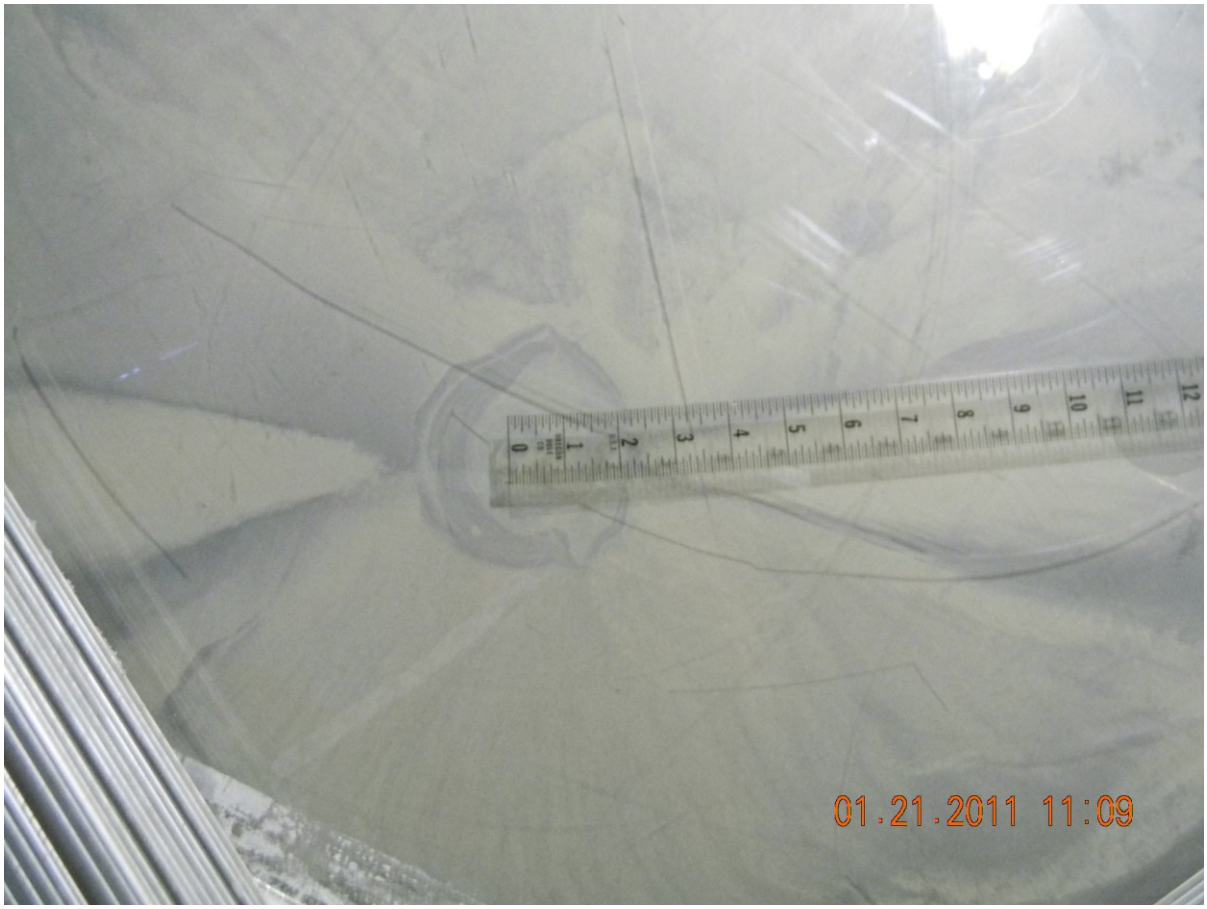

Figure 8: MJP Non-rotating Jet Mixing, 7.0 Pa Simulant, Test 4

The non-rotating jet cleaning radius test was conducted at three different flow rates 4 gpm, 6 gpm, and 8 gpm as shown in Table 6. On all tests the contents of the tank was mixed at 10 gpm or higher for 30 plus minutes. To begin the test, the flow rate of the MJPs was reduced to about 1 gpm. When the flow rate decreased, the rotation of the MJP was also stopped when one of the jet nozzles was pointing to the dead zone (farthest radial point on the tank wall from the jet). The MJP flow rate was than increased to the test flow rate. Readings were taken until the cleaning radius no longer increased Normally the maximum distant that the jet would clean at a given velocity was obtained in approximately three minutes. Readings would continue to be taken for an additional three to four minutes at that velocity.

Table 6: MJP Non-rotating Jet Cleaning

Test #	Slurry	MJP @ 4 gpm Inches	MJP @ 6 gpm Inches	MJP @ 8 gpm Inches
3	14 wt% Kaolin /5 wt% SS	15 ½	19 ¾	22
4	23.4 wt% Kaolin /5 wt% SS	9 ¾	15 ½	16
6	52 wt% Glycerol /5 wt% SS	15	18 ½	22
9	19 wt% Kaolin /5 wt% SS	11	13 ¾	17

The cleaning radius of the fixed jet was increased when the simulant had little to no yield stress. Comparing the cleaning radius of Test 4 (YS = 7.0 Pa) to Test 6 (YS = 0), the glycerol which had no yield stress had the larger cleaning radius, cleaning the entire MDT, a distance of 22 inches. In the discussion below on the cleaning radius with rotating jets, it is apparent that a jet in a fixed direction gives longer cleaning radius than the jets rotating at 1.6 RPM in this study. With this information of the fixed-direction jet, the full-scale tanks could have the MJP jet nozzles oriented to point at the dead zones to potentially remove mounds of particles that are settled in these areas.

Transfer Results

For the mixing/transfer demonstrations with rotating jets, the simulant in the MDT was mixed at two different flow rates supplied to each Mixer Jet Pump, 8.0 gpm (velocity, 22.4 ft/s/nozzle) and 10.0 gpm (velocity, 28 ft/s/nozzle). Figure 9 shows the flow rate to each MJP (8 gpm) and the transfer flow rate (0.58 gpm) for the Test 6 using glycerol. This is a typical flow curve for the tests conducted in Phase III where the MJPs were operated at 8 gpm and shows that velocities were constant except at the end.

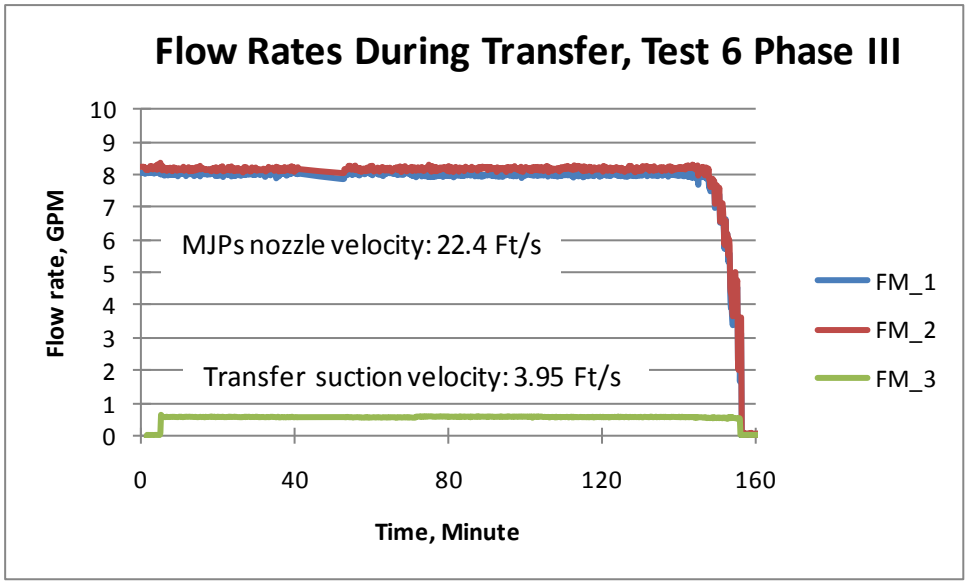

Figure 9: MJPs and Transfer Flow Rates, Test 6

The MJPs continued to mix the contents of the MDT while the batch transfers were being made. As depicted in the curve, the transfer pump was not shut down between batches. Each batch took approximately 25 minutes and all six batch transfers were completed in about 150 minutes. Figure 10 gives a more detailed look at a typical transfer during Phase III. In this figure, a 1.6 Pa kaolin/SS slurry is being transferred at a target of 0.58 gpm from the MDT to the Receipt Tanks. This flow rate results in a suction velocity of 3.95 ft/s at the inlet located a ¼" off the bottom of the MDT. During the Batch 6 transfer mixing becomes very poor inside the MDT due to low level of the slurry. The plot shows the transfer flow rate falls off

due to pulling in air, causing the 6th transfer to end before the full batch volume is pumped from the tank. This is typical of most all Batch 6 transfers for all phases of testing.

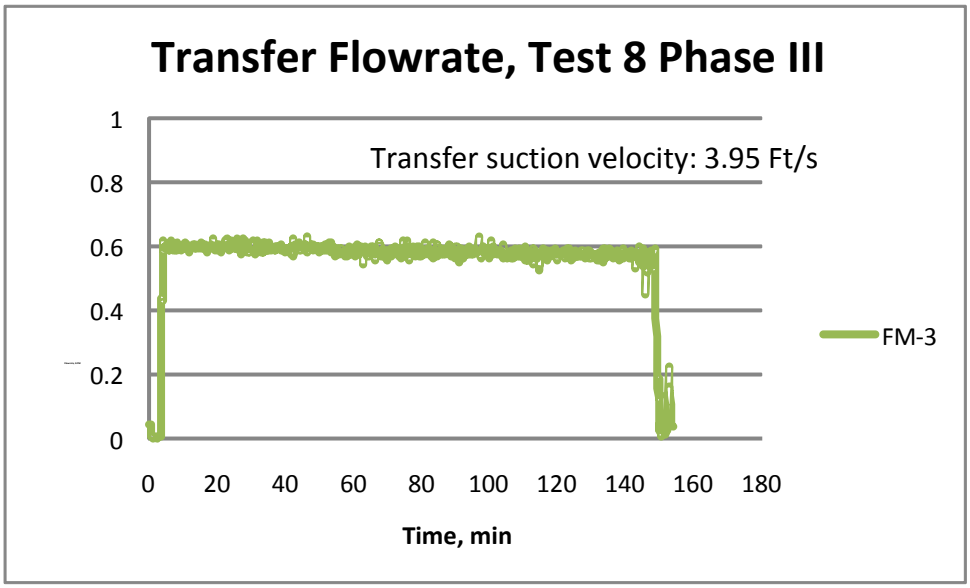

Figure 10: Transfer Flow Rate, Test 8 Phase III

Figure 11 is a picture of Test 4 showing the SS settled out in the bottom of the RTs after TSPP had been added to the slurry and mixed. There was markedly less consistency of SS between batches in this test in comparison to nearly equal amounts of SS in each Receipt Tank in the water test (Test 1). Note that the volume of SS as measured by visual observation of the SS depth in the RTs decreases with each batch transfer. This was due to the transfer pump beginning to fail. On Test 4 the pump motor speed controller had to be adjusted to attempt to keep the flow rate at 0.58 gpm since the flow rate was constantly falling off. During this time there were periods where the technician allowed the flow rate to droop below 0.58 gpm. At the end of the Test 4 the transfer pump was rebuilt and it was found the pump housing was packed with SS particles.

Figure 11: SS Settled from Kaolin in the Receipt Tanks of Test 4 (TSPP Added)

As seen in earlier tests, the transfer of solids on Batch 6 was impacted by poor mixing in the MDT when the liquid level was low. This is also evident in Receipt Tank 6 (far right) in Figure 11 for Test 4 where the solids level can be seen and is less than a complete transfer (less than 14.3 gal).

Figure 12 shows the SS settled out in the bottom of the Receipt Tanks. The picture on the right is a close-up of the settled SS in RT-3 from Test 5.

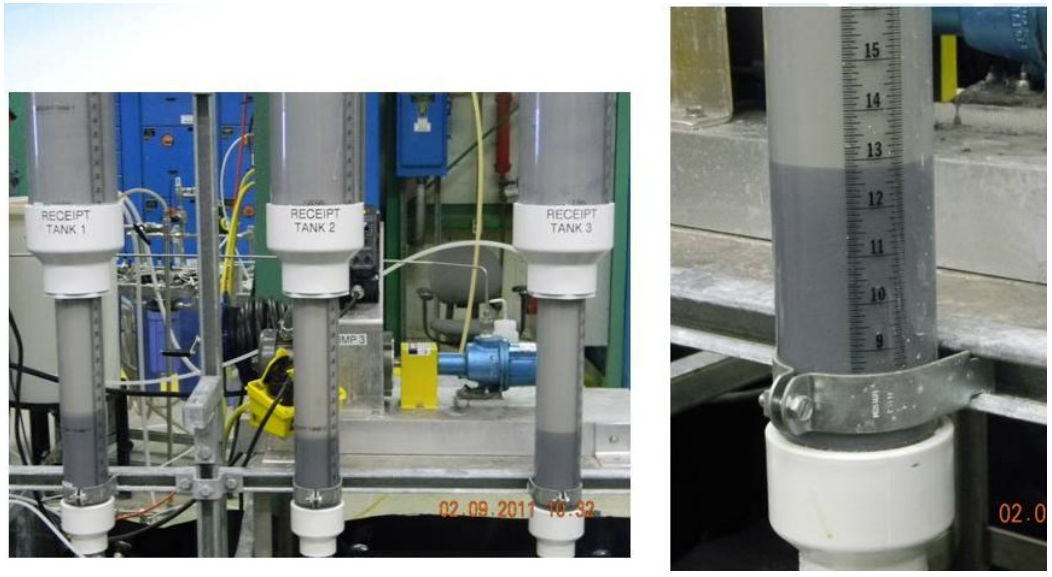

Figure 12: SS Settled to Bottom of RTs, Test 5 (TSPP added)

Table 7 gives the measured height of the SS settled to the bottom of each Receipt Tank for each tests conducted during Phase III. For tests using 19 wt% and 23.4 wt% kaolin simulants, which have a sufficient yield stress to stop the settling of the SS seed particles, TSPP was added in the RTs after the transfers were completed to eliminate the yield stress and allow the SS seed particles to settle quickly to the bottom of the Receipt Tanks. TSPP contaminated slurries were not reused except for Test 5A.

Table 7: SS Transferred to Receipt Tanks

	RT-1 inches	RT-2 inches	RT-3 inches	RT-4 inches	RT-5 inches	RT-6 inches	RMS Deviation (%)
Test 1	6 3/4	6 3/4	6 3/4	7	7 1/4	8 1/2	2.9
Test 2	7 3/4	7 3/4	7 3/4	7 3/4	7 3/4	7 3/4	0
Test 3 *	6 13/16	8 3/4	7 3/4	8	7 3/4	3 ++	7.9
Test 4 *Δ	13 3/8	12 1/2	11 15/16	11 3/16	9 3/4	8	10.5
Test 5 *	13 3/4	12 1/4	12 13/16	12 1/2	13 3/8	9 7/16	4.3
Test 5A	7 1/4	8 7/8	8	8 5/8	8	9 1/4	7
Test 6	6	6	6 3/8	7	7	8 1/2	7
Test 7	9 1/16	9 3/4	8 15/16	8 5/8	9 7/16	10 3/4	8.6
Test 8 *	10 5/8	10 1/4	9 3/4	10 1/8	9 13/16	7 3/4	3.1
Test 9 *	11 7/16	11 11/16	12 ½ ¥	11 15/16	11 1/2	8 1/4	3.3

* TSPP added to receipt tanks
++ Estimated height of SS in reducer
Δ Transfer pump started to fail due to impeller wear
¥ RT was filled to 15.9 gallons
RMS - root means square

The tests with the higher yield stress had the most effective batch transfers of SS solids out of the MDT, Tests 4 (23.4 wt%/SS), 5 (23.4 wt%/SS), 8 (19 wt%/SS) and 9 (19 wt%/SS) as shown in Figure 13. This plot is a comparison of SS transferred to the Receipt Tanks for tests using kaolin/SS (cohesive simulant) and the water/SS test. The data in the plot is from Table 7. For clarity, due to the inconsistency of Batch 6 transfers, Batch 6 data was not plotted. The consistency of the SS transferred from batch to batch was good except for Test 4.

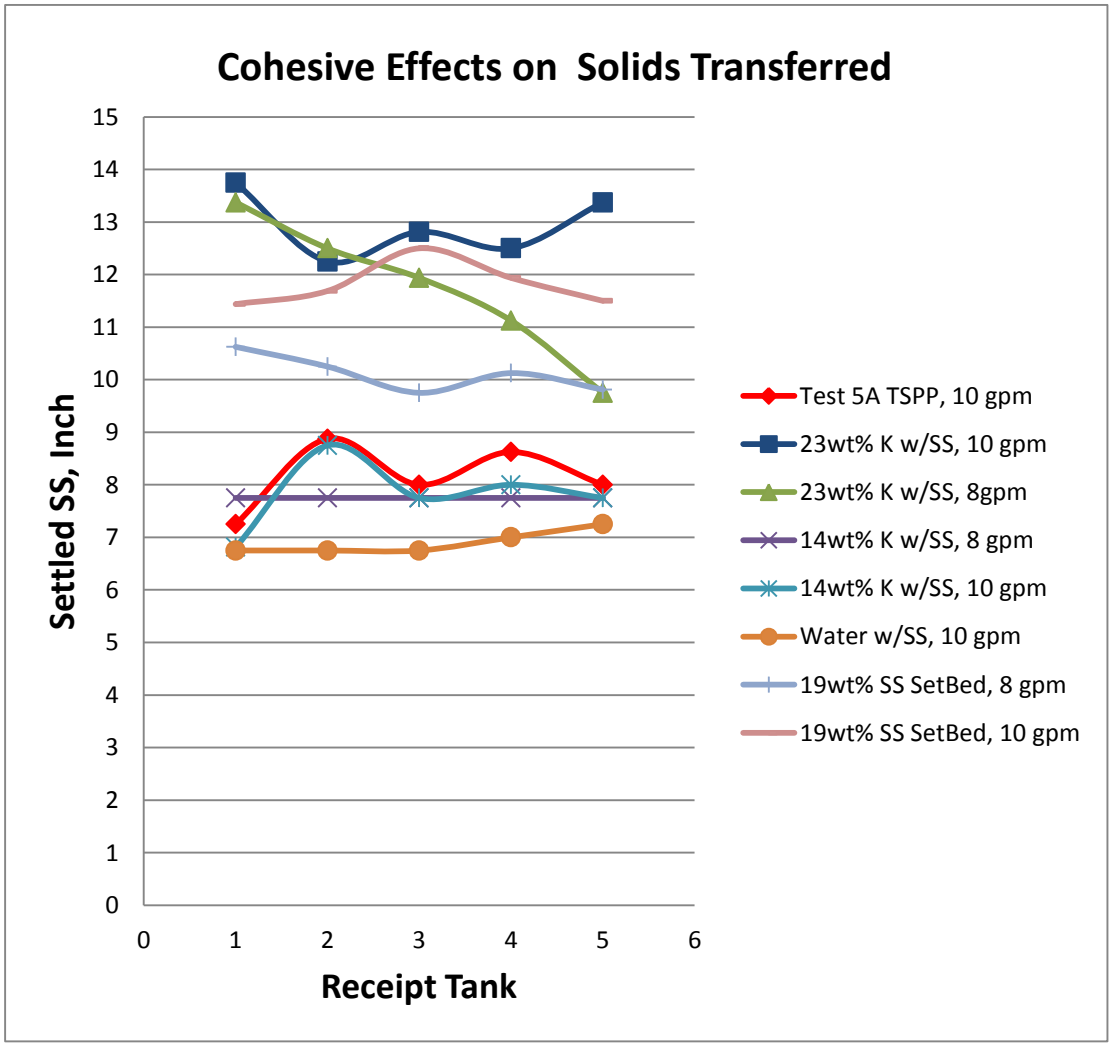

Figure 13: SS Particles Settled to Bottom of Receipt Tanks

The plot shows that batch transfer of solids was less effective when only water was used as the carrier fluid. However, as the wt% of kaolin was increased (increasing the YS of the batch) the efficiency of transferring solids also increased. This plot suggests that when testing with water as the carrier fluid, the test is conservative on the transfer of solids when compared with a carrier fluid with a yield stress which is more efficient transferring solids. The conclusion from this plot, that water always transfers less seed particles, and is conservative by this metric, when compared to fluids with a higher yield stress and/or higher viscosity at the same mixing/transfer parameters.

The root means square (RMS) deviation in Table 7 was calculated by determining the average height of SS for the first 5 batches (the 6th batch was neglected). Then the difference between each batch and the average for the test divided by the average for the test, that number was then squared as shown in the following equation.

$Batch_i$ difference = $((B_i - B_{avg})/ B_{avg})^2$

Those squares were then averaged and the square root was taken to determine the RMS deviation for each test:

RMS = SQRT((Average B_i : B_N))

Test 4 had a 10.5% RMS deviation of transferred solids due to the transfer pump wear during this test. If this outlier is excluded, the other tests shows an average of 5% RMS.

Figure 14 is a plot of the average height of SS solids transferred to the RTs as a function of the Bingham yield stress of the slurry. The plot suggests that the average transfer of solids always increases with increasing yield stress. Also, more vigorous mixing in the MDT (8 gpm vs. 10 gpm flow rate to the MJPs) improved the solids transfer of the cohesive simulants to the RTs.

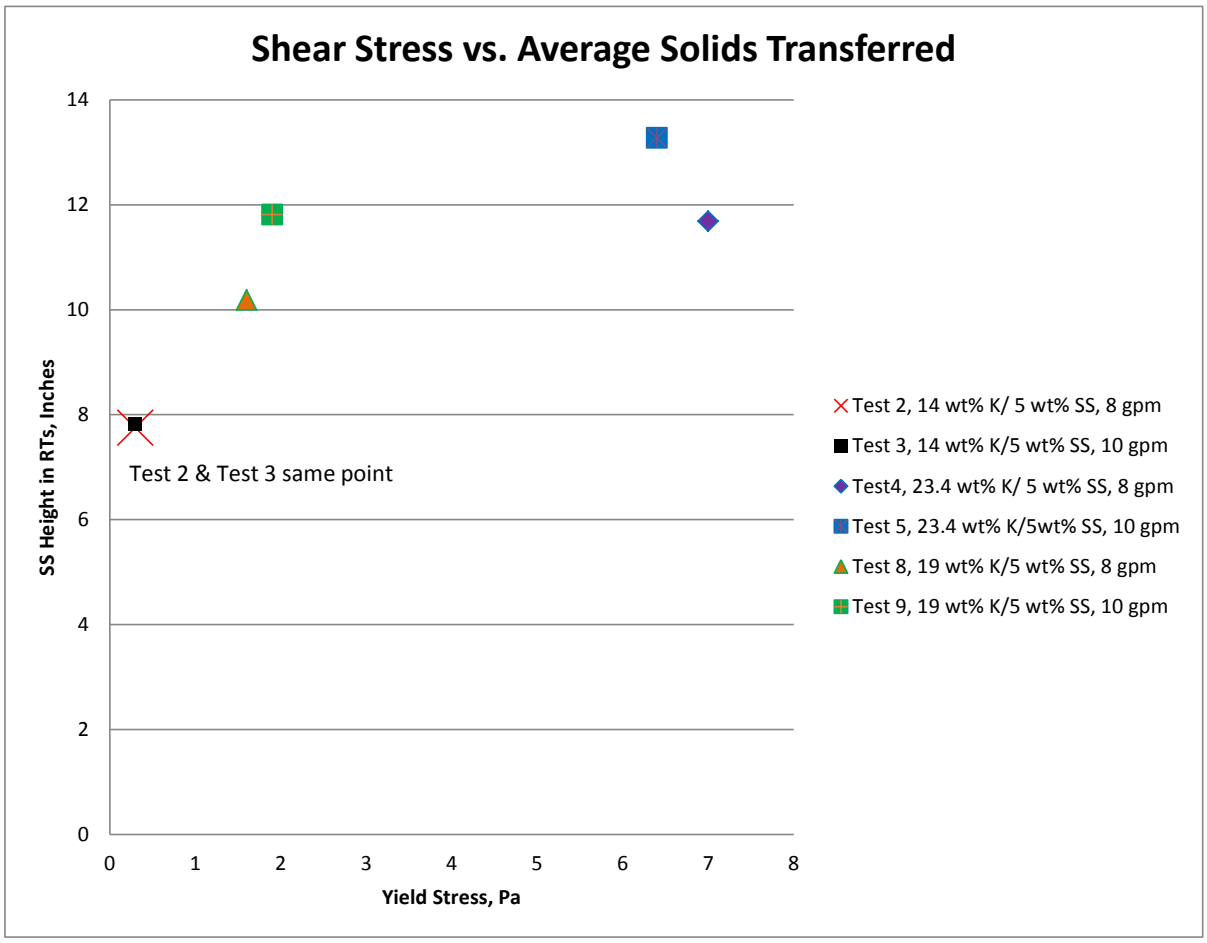

Figure 14: Shear Stress of Simulant on Solids Transferred

Figures 15 and 16 are plots of the average height of SS solids transferred as a function of the viscosity carrier fluid viscosity (or Bingham consistency) when the MJPs are operating at 8 gpm and 10 gpm, respectively. In these plots 52 wt% Glycerol /5 wt% SS (yield stress = 0) is compared to 19 wt% kaolin /5 wt% SS and 23.4 wt% kaolin /5 wt% SS. The average height of SS solids for each point is for the first five batch transfers (data from Table 7). As shown in Figure 15, the viscosity of the glycerol/water mixture falls in between the viscosity of the two kaolin slurries. Because the viscosities are nearly matched, the key difference between the two slurries and the glycerol/water mixture is that the slurries have a yield stress. As discussed previously, the yield stress is due to the cohesive particle interactions in the slurries. The results show that the glycerol/water mixture always had less SS seed particles transferred than the two kaolin slurries for both the 8 gpm and 10 gpm MJP operation. The result suggests that increasing the yield stress of the carrier fluid, which corresponds to greater cohesive particle interactions, gives better transfer of dense SS particles.

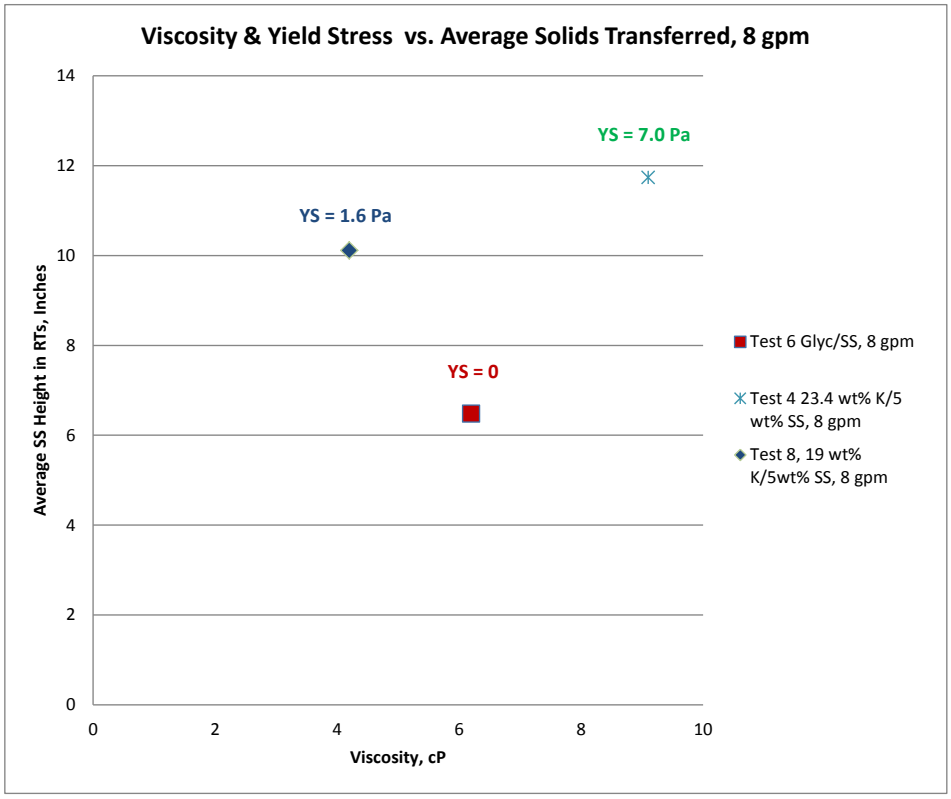

Figure 15: Viscosity & Yield Stress vs. Average Solids Transferred, 8 gpm

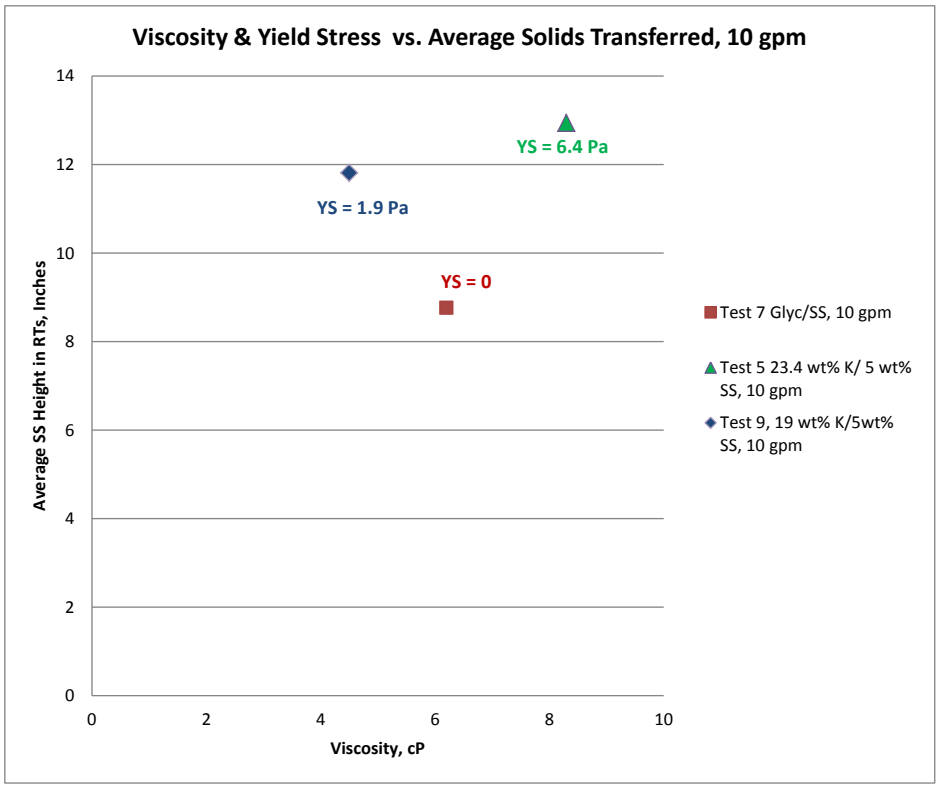

Figure 16: Viscosity & Yield Stress vs. Average Solids Transferred, 10 gpm

Comparing test results with slurries with Bingham yield stresses of 1.6 Pa to 7 Pa to a Newtonian glycerol/water mixture with a viscosity approximately equal to the Bingham consistency (viscosity) of the slurry, the slurries with a yield stress had a significant increase of solids in the batch transfers. This finding shows that cohesive particle interactions, which impart a yield stress to the slurry, result in an overall increase in seed particle suspension and transfer, which is an improvement in mixing performance.

At the end of the six batch transfers there was always at least ¼" to ½" of slurry left in the MDT with solids in the two dead zones. Figure 17 shows the extreme of solids left in the dead zone of the MDT. The picture on the left depicts SS solids in the dead zone during mixing the water/5 wt% SS particles. In this picture the MJPs were operating at 10 gpm (28 ft/s), rotating at 1.6 rpm. The poor mixing that the carrier fluid (water) created allowed a large dead zone to form while the MJP operated at 28 ft/s. As the liquid level was reduced by the transfers, the solids in the dead zone flattened out. The solids in the dead zone flatten out as the liquid level in the tank decreased. This is due to the surface motion of the carrier fluid as the mound of particles surfaced above the liquid level. The picture on the right shows the dead zone at the end of the six batch transfers. The dead zone on the opposite wall of the MDT has essentially the same amount of SS solids as shown in this view.

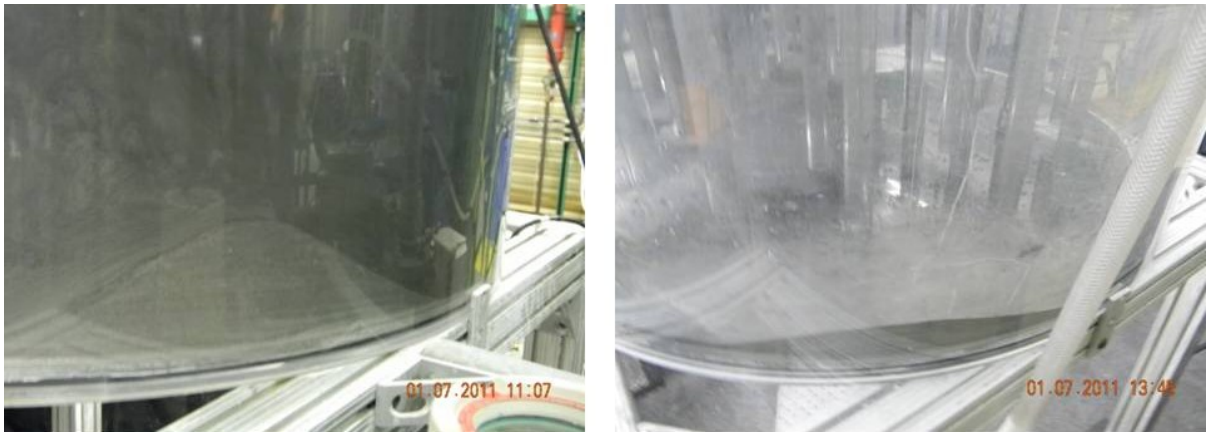

Figure 17: MDT Dead Zone Particles in Water, Test 1 Phase III

Figure 18 visually shows no SS particles in the dead zone while mixing with 1.9 Pa kaolin slurry. A view from the underside of the tank, the SS was mixing into the slurry and not falling out in the dead zones. The picture to the left shows that there is essentially no dead zone after 30 minutes of mixing. The picture on the right shows a top view with approximately ½" of kaolin slurry and very few solids in the dead zone. The slurry is well below the obstructions (air lift circulators). There are no visual signs of SS in the two dead zones (occurring at maximum distance from MJP center lines). But due to the poor mixing when the liquid level drops to about 2", there would always be a small amount of solids, usually the larger, denser SS particles that could be seen from the underside of the tank.

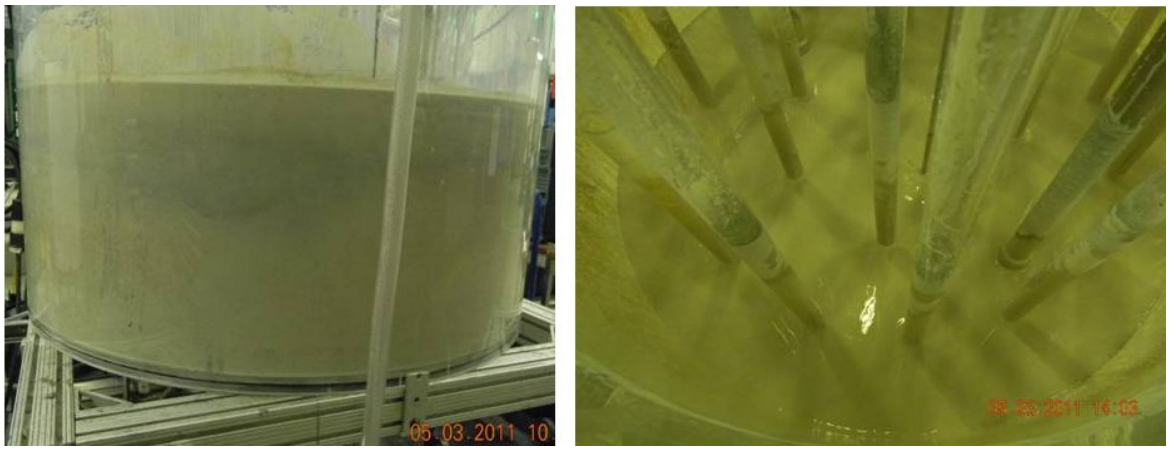

Figure 18: MDT Dead Zone Particles in 1.9 Pa Kaolin, Test 9 Phase III

As described previously for Test 8 and Test 9, the SS was not initially uniformly mixed into the kaolin as in the previous tests. For these two tests, the 5 wt% SS with about 3 gallons of kaolin slurry was placed in the MDT as a settled bed. This resulted in a one inch bed settled

solids as shown in Figure 19. This test represents a more significant challenge to mobilize and distribute the seed particles throughout the MDT during the mixing period prior to the batch transfers.

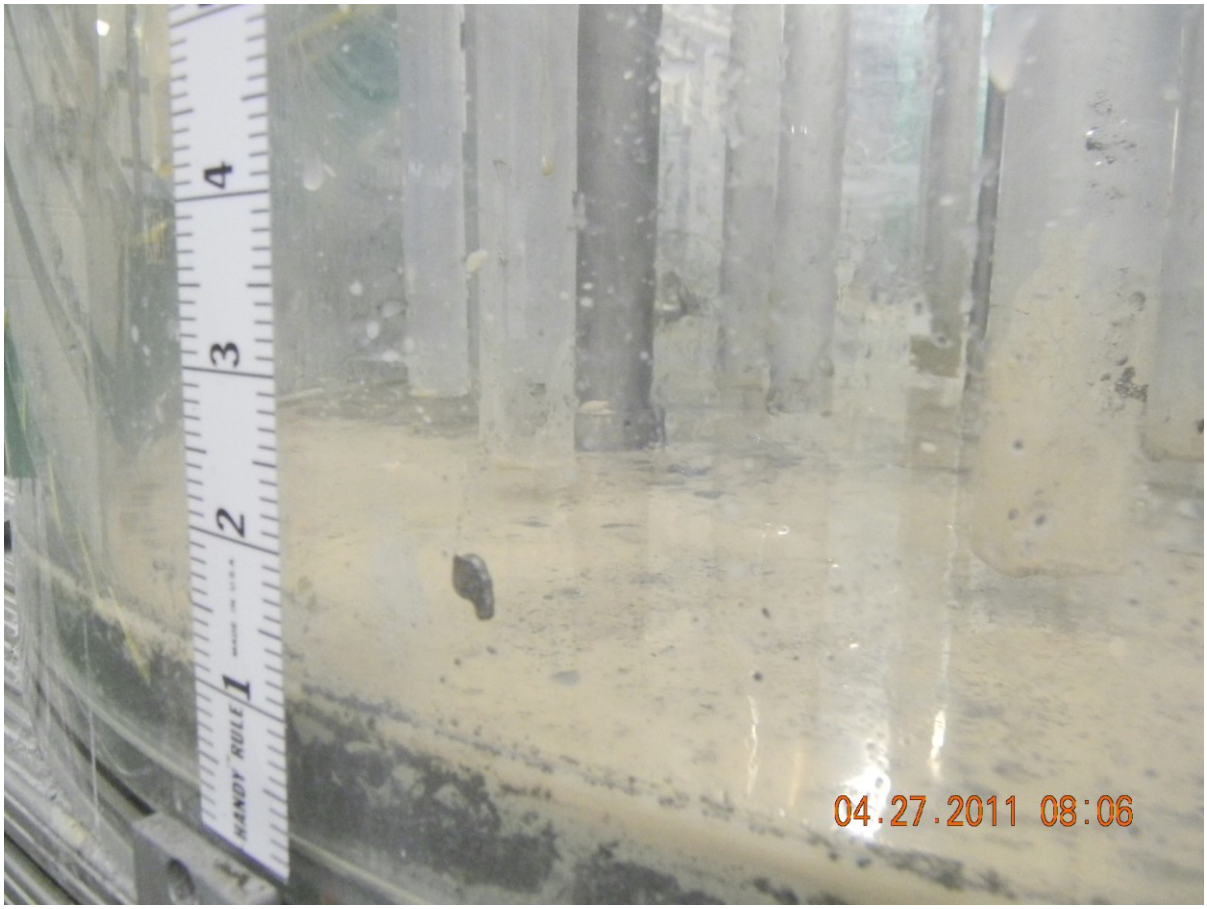

Figure 19: MDT Preset 1" Settled Solids Bed, Test 8

The MJPs performed well for mixing the settled SS into kaolin for both Tests 8 and 9. Within the first 30 minutes of mixing, the SS from the initial layer was mixing throughout the kaolin. The batch transfer of solids to the RTs showed a higher amount of SS being transferred in comparison to water, which is good transfer based on this metric. Figure 20 gives a visual indication of the solids settled for Test 8 after the 600 ppm of TSPP was added to the RTs. In the bottom clear section of the RTs is the darker SS. There is a defined dark line in each RT. Above the dark SS line, is 1.6 Pa kaolin which does not settle in 24 hours. RT-6 was not a complete transfer.

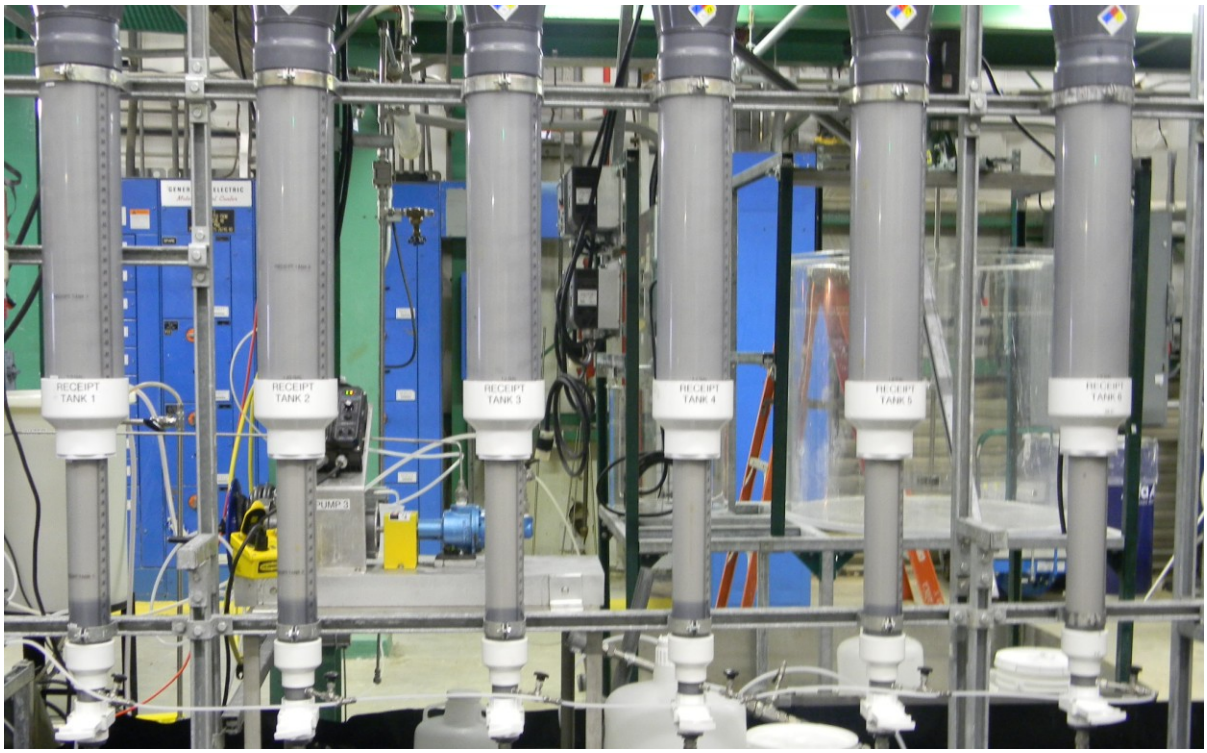

Figure 20: Settled Solids in RTs, Test 8 Phase III

Figure 21 is a close-up photo of the SS in RT-3, Test 9. The view shows that there is a faint line about a 1" above the defined SS line. This faint line could be seen on the first five RTs of Test 9. This faint line was not noticeable on the other tests. This line is possible associated with a portion of the SS seed particles that are smaller than average, but no specific evaluations were done to explain this observation.

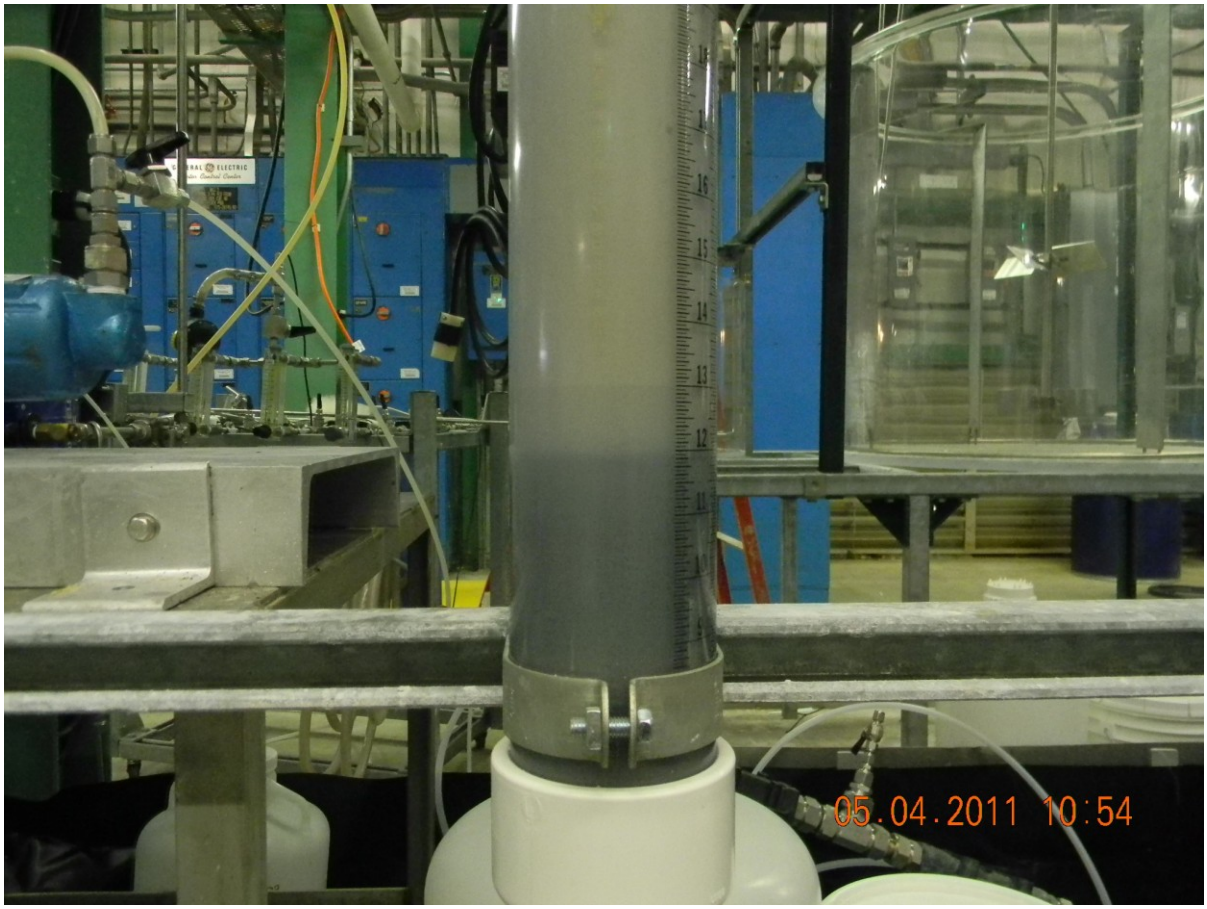

Figure 21: Close-up View of Settled SS in RT 4, Test 9 Phase III

The primary purpose of conducting tests with glycerol/water mixtures was to compare mixing and batch transfer results with cohesive slurries with similar viscosity. These data can also be compared with water to demonstrate the effect of viscosity on mixing/batch transfers. Two mixing/transfer demonstrations with glycerol were conducted. The same batch of glycerol/SS was used for both tests. It was found the glycerol had a small improvement on the transfer of solids when compared to the water/SS at the same MJP flow of 10 gpm as shown in Figure 22. Testing suggests that the higher viscosity of the glycerol (6.2 cP) improved the transfer of solids when compared to water. The testing also suggest that water is conservative (less SS seed particles transferred) when compared to a carrier fluid with a greater viscosity. Using a simulant with a greater viscosity would result in a better transfer of solids when the mixing/transfer parameters are the same.

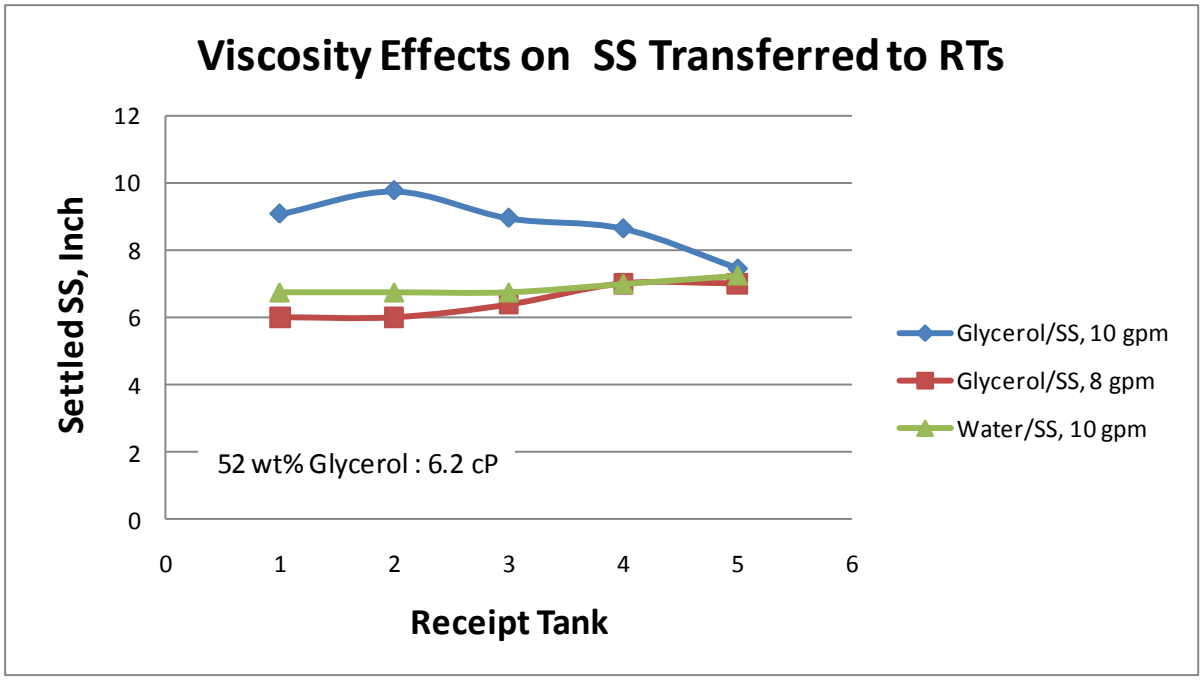

Figure 22: Viscosity Effects on Batch Transfers

Figure 23 shows the effect of the Bingham consistency (viscosity) on the average height of SS solids transferred to the RTs. In this plot the MJPs are operating at 8 gpm (the water result at 10 gpm is included for comparison). The average height of SS solids for each point is for the first five batch transfers (data from Table 7). Figure 24 is essentially the same plot except that the MJPs are operating at 10 gpm. Batch 6 was not plotted because of inconsistency of this transfer discussed earlier. Comparing the average height of SS transferred to the viscosity of the carrier fluid, the SS was consistently transferred better when the carrier fluid had a viscosity higher than water. It is important to note that these slurries also had a yield stress, and the increase in the transfer of SS particles is also affected by the yield stress.

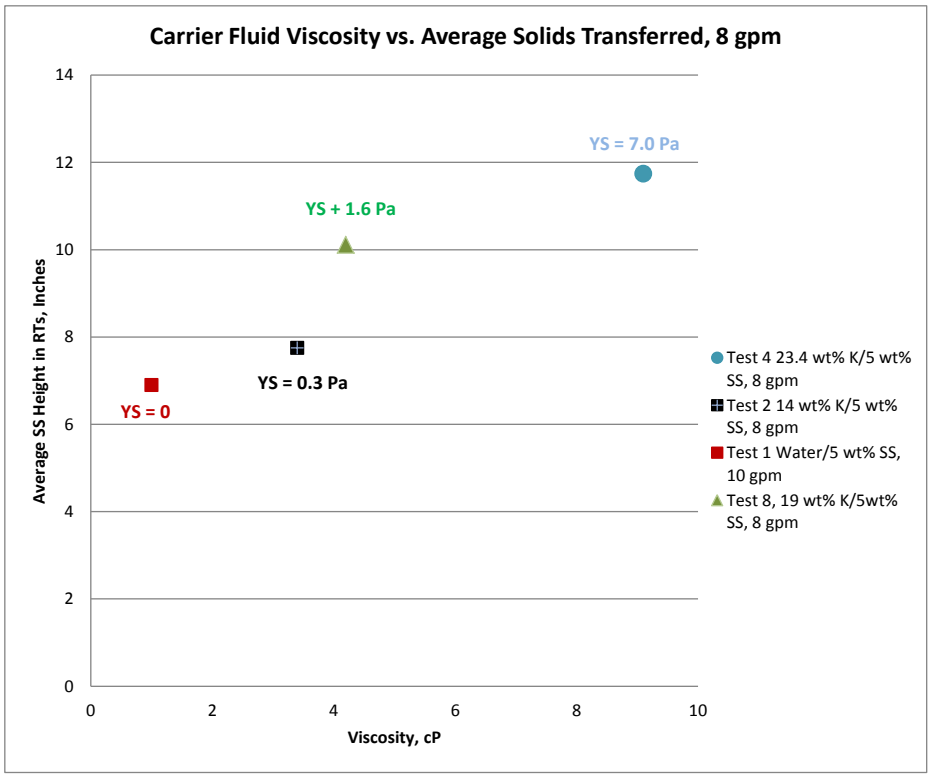

Figure 23: Effect of Carrier Fluid Viscosity on the Average SS Height in the Receipt Tanks for MJP Flow of 8 gpm

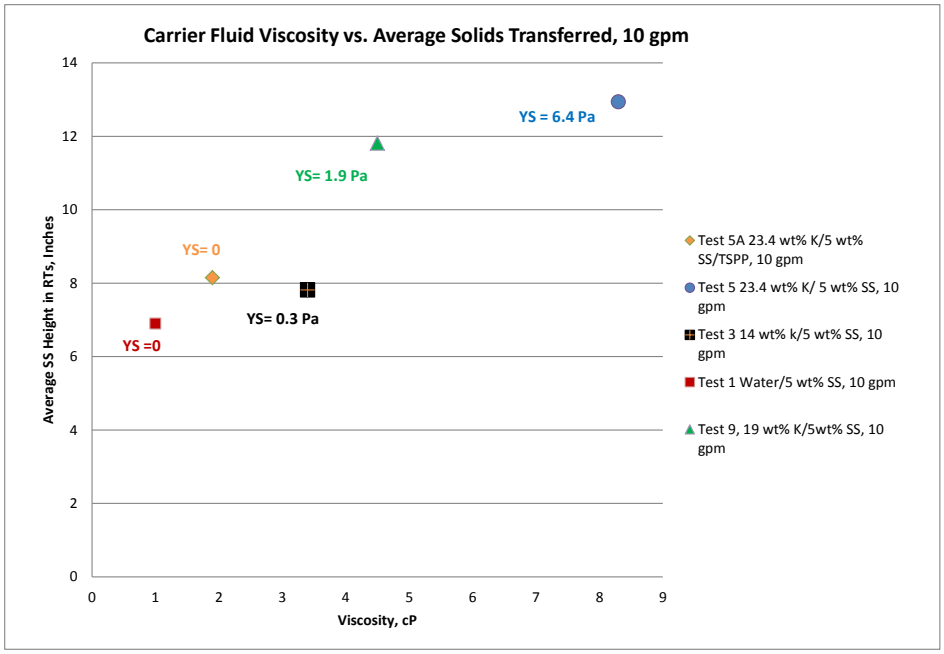

Figure 24: Effect of Carrier Fluid Viscosity on the Average SS Height in the Receipt Tanks for MJP Flow of 10 gpm

As the yield stress of the slurry increases the observed mixing in the MDT decreases. However, the total batch transfer of seed particles always increased with an increase of yield stress. When mixing slurries with MJPs, it is more difficult to suspend particles from the tank bottom with increasing yield stress, but the particles stay suspended to a greater degree once lifted from the tank bottom. The combined effect of increasing the yield stress is an increase in the transfer of seed particles.

Cleaning Radius Results for Rotating Jet

The cleaning radius of the rotating MJP at various flow rates was investigated. Figure 25 is an image of a rotating jet nozzle at 3 gpm to the MJP (8.4 ft/s/nozzle) during Test 6. In this picture, the dark area is where the jet is cleaning the bottom of the tank. The grayish area is where the SS is settling out of the glycerol. The glycerol/SS had a totally different visual effect when compared to the kaolin/SS. When the SS was added to the glycerol the carrier fluid (glycerol/water) took on a dark black color and the settled SS looked gray. Where with the kaolin/SS, the carried fluid (water) looked gray and the settled SS appear black.

Figure 25: Rotating Jet, Low Velocity Cleaning Radius, Test 6

The cleaning radius measurements were done by viewing the operation of the MJPs from the underside of the MDT (transparent bottom) while varying the MJP flow rate. Before the start of the cleaning radius test, the contents were mixed for approximately 30 minutes then the flow was decreased to 1 gpm. Once the flow was at this flow rate for one minute, the cleaning radius was measured. The flow rate was then increased in 1 gpm increments up to 10 gpm. Measurements were typically made after about 3 jet rotations because the cleaning radius was changing slowly, or not at all, with additional rotations.

Figure 26 gives the rotating cleaning radius for the range of nozzle velocities tested. On most tests a cleaning radius could not be determined when the flow rate was set at 2.8 ft/s/nozzle (1 gpm/MJP). This is due to the low velocity not having the energy to move solids around on the bottom of the tank. The plot indicates that the 23.4 wt% kaolin/ 5 wt% SS had the smallest cleaning radius at each velocity except for 5 ft/s. At 28 ft/s/nozzle the 14 wt% kaolin/ 5 wt% SS had the largest cleaning radius at a little over 16". In general, the cleaning radius progressively decreased with increasing slurry yield stress. An important comparison is that the 6.2 cP glycerol/water Newtonian fluid has cleaning radius equivalent to the 19 wt% kaolin (1.9 Pa, 4.5 cP) of Test 9, particularly at the high jet velocities.

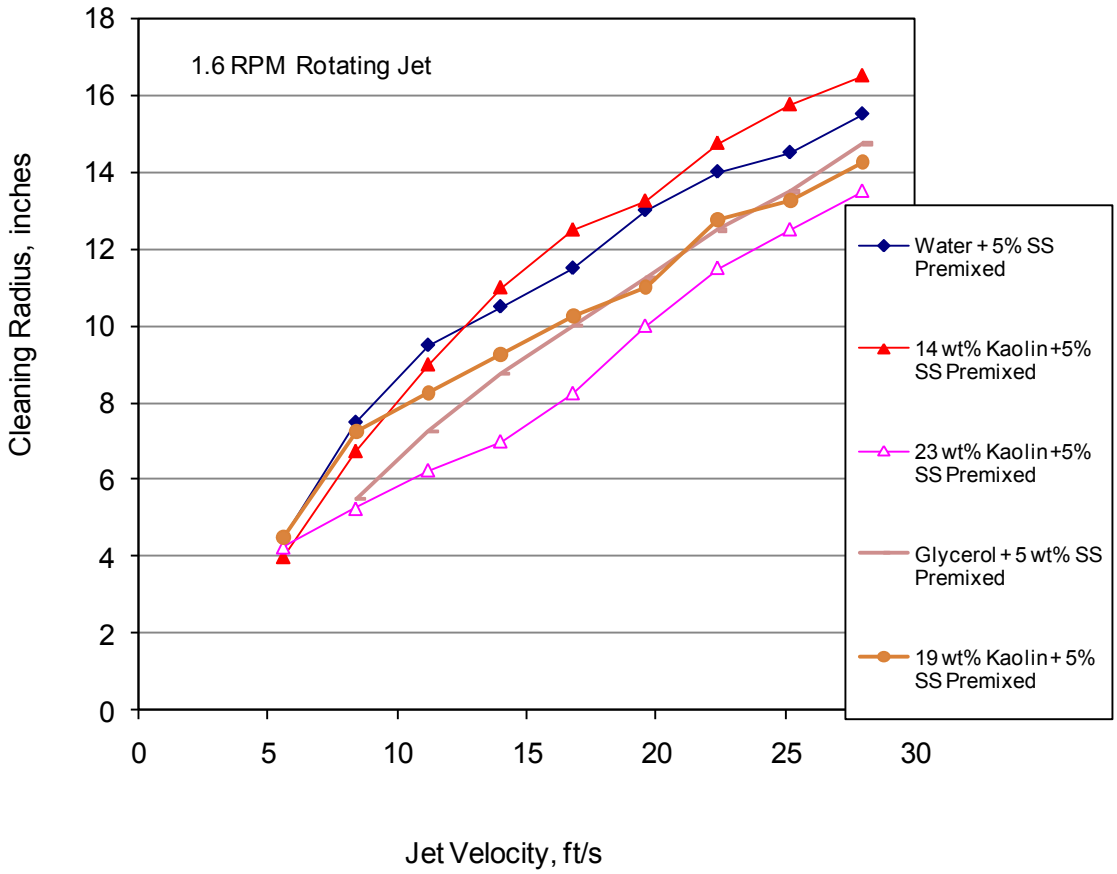

Figure 26: Rotating Jet Cleaning Radius

A series of essentially identical cleaning radius tests showed repeatable for three tests conducted on the premixed 14 wt% kaolin/ 5 wt% SS. Figure 27 shows that for these three tests, the cleaning radius was essentially repeatable, particularly at the higher velocities that are the important range for testing the MDT. The difference in the three cleaning curves is at low velocities likely due to jet not being sufficiently turbulent.

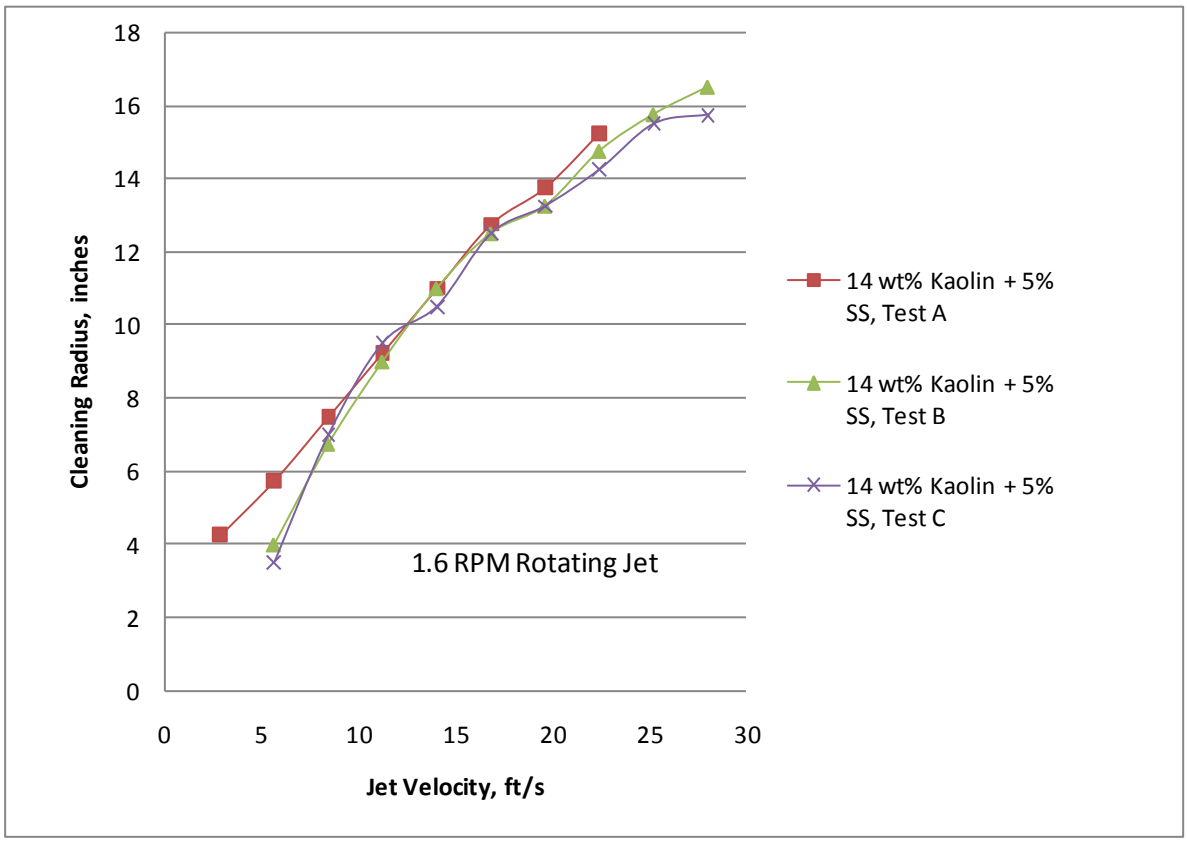

Figure 27: Rotating Jet Cleaning Radius Repeatability

The cleaning radius of a MJP jet can also be affected by whether or not the contents of the tank had settled undisturbed for some period of time. Figure 28 compares the cleaning radius of the jet for a settled tank and a premixed tank. In this plot, the settled tank had been allowed to settle undisturbed for three days before this cleaning radius test. The plot shows it takes roughly 2 ft/s greater jet velocity to start the erosion of settled solids off the bottom of the tank after three days of settling. With the settled solids test, a cleaning radius was not determined from the underside of the tank until 11.2 ft/s/nozzle (4 gpm/MJP). A premixed tank was where the MJPs flow rate was increased until the settled solids were suspended off the bottom with no dead zones. With the premixed MDT on Test C, the cleaning radius was determined at 5.6 ft/s/nozzle (2 gpm/MJP) and higher velocities. At the higher jet velocities the cleaning radii for the settled and non-settled tests were similar.

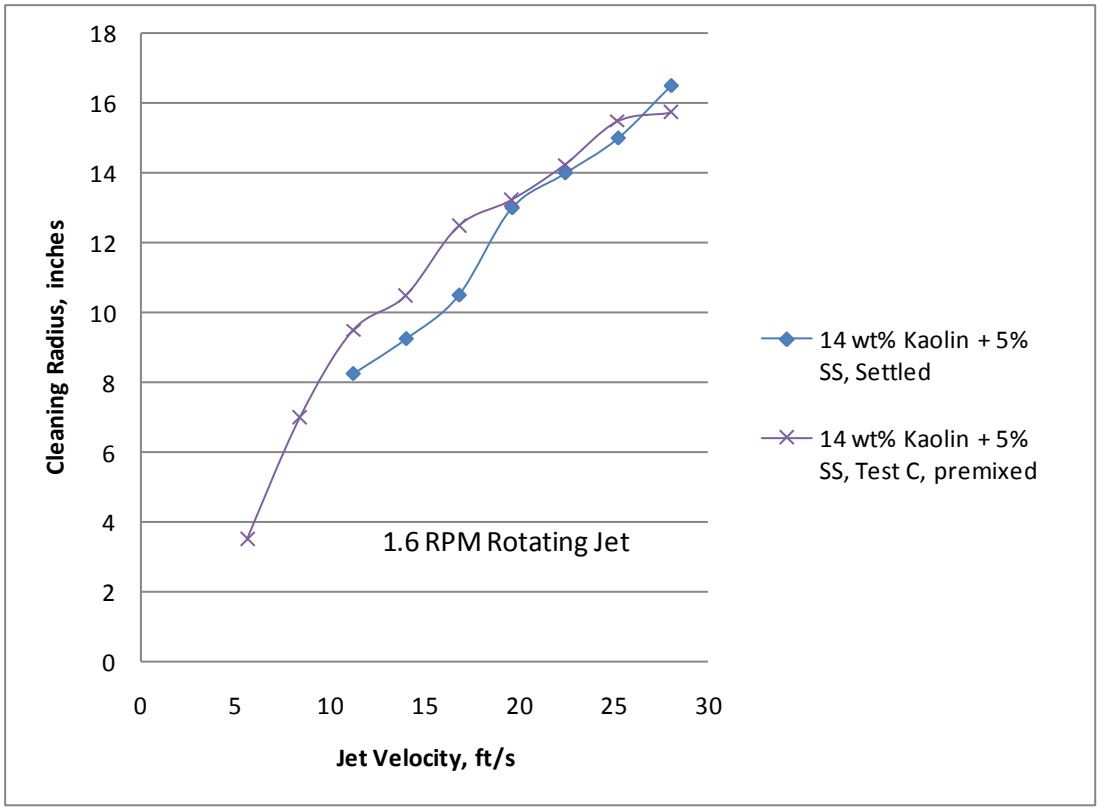

Figure 28: Rotating Jet Cleaning Radius Settled vs. Premixed Tank

At the higher velocities, the rotating jet cleaning radius test may be skewed due to the method the test was conducted. As the flow rate was increased one gpm at a time and a reading taken one minute after the flow had been set, a larger dead zone of SS particles was building up just beyond that cleaning radius. As SS particles build up in an area, it takes more energy to remove the pile of particles. For instance on Test 9, after the MJPs were operated at 10 gpm (V = 28 ft/s) for 30 minutes, the cleaning radius was 19 inches. When the flow rate was reduced to 1 gpm and stepped up incrementally to 10 gpm over about a 20 minute period, the cleaning radius at 10 gpm was 14 ¼". At the end of the cleaning radius test, the contents of the MDT were mixed for approximately 20 more minutes at 10 gpm before beginning Batch 1 transfer, and the cleaning radius returned to 19 inches. Figure 29 shows the cleaning radius at 19 inches in this test. The picture also shows the region of the dead zone in this tests, which was between 19" and 21". Visually, there is mixing at the wall with a small dead zone that acts as an island. There was good motion of slurry on all sides of the dead zone.

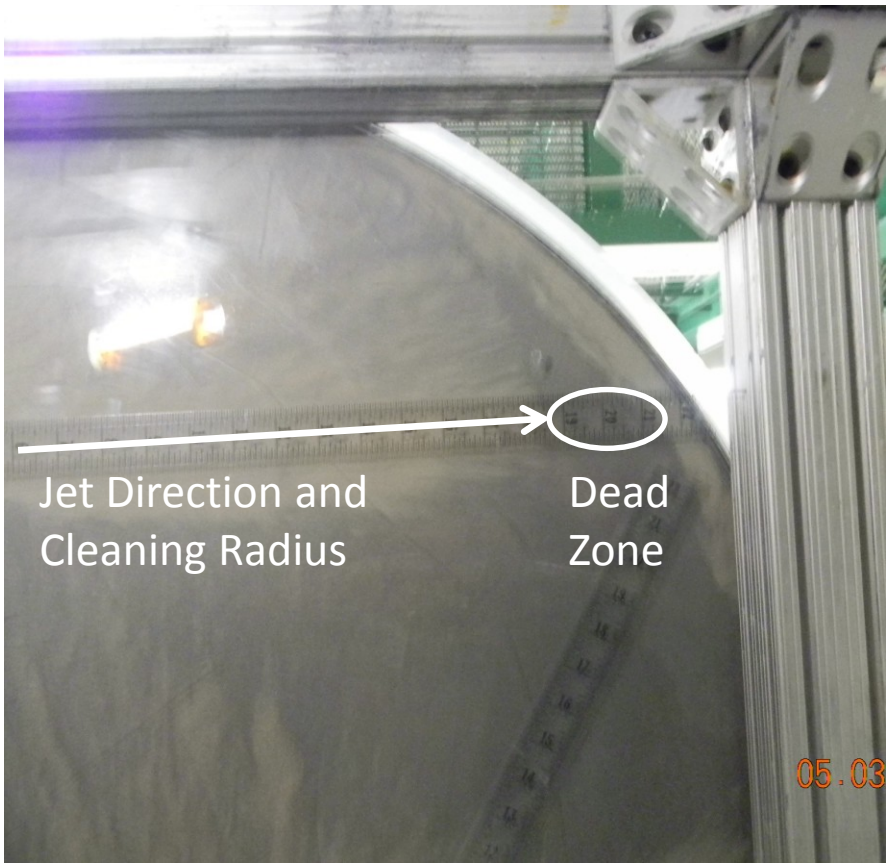

Figure 29: Rotating Jet Cleaning Radius after 30 min, Test 9

The cleaning radius of the MJPs is impacted by the rheology of fluid being mixed. From this study one can conclude that as the MJP cleaning radius decreases as the yield stress of the fluid being mixed increases.

Dimensional Analysis

The yield stress in the slurry affects the suspension and settling of the SS seed particles and the overall fluid motion in a number of ways. It is desired to quantify, to the degree possible, how broadly the results obtained in this study can be applied to the full-scale mixing behavior of DST waste with cohesive slurries that exhibit a yield stress. Dimensional analysis is a useful tool for making this evaluation. Previous studies have applied dimensional analysis to jet mixing of DSTs with horizontal jets (Bamberger et al. 1990 [7]) and the similar problem of vertical pulsed jets (Meyer et al 2009 [8], Bamberger et al. 2005 [9]). There are a number of dimensionless parameters that are identified, but for our evaluation here we will focus on how switching from a Newtonian liquid to non-Newtonian fluid that follows the Bingham model changes the analysis.

In dimensional analysis, the choice of the specific dimensionless numbers to use is not unique. For evaluating particle settling behavior in a Newtonian fluid, a common dimensionless group to use is the Archimedes number given below.

$$\mathrm{Ar} = g d_p^3 \rho_l (\rho_p - \rho_l)/\mu^2$$

In comparing Newtonian and Bingham fluid models, the Newtonian fluid is characterized by a single parameter, the viscosity, while the Bingham fluid has two parameters – the yield stress and consistency (plastic viscosity). Applying dimensional analysis, one additional dimensional group is needed to describe the behavior of a Bingham fluid in comparison to a Newtonian fluid. Again, the selection of dimensionless groups is not unique and for this evaluation we will replace the Archimedes number with yield Reynolds number and the gravity yield parameter shown below.

Yield Reynolds Number – $\mathrm{Re}_\tau = \rho U_j^{\,2}/\tau_y$
Gravity Yield Parameter – $Y_G = \tau_y/g(\rho_p - \rho_l)d_p$

The yield Reynolds number is typically used to quantify the size of a cavern, which is defined as a region where the jet causes fluid motion, but outside of which the Bingham fluid remains stagnant due to the yield stress. The gravity yield parameter is often used to quantify the transition between particles that will sink due to gravity in a fluid with a yield stress or not (Chhabra 1993).[10]

Figure 30 is a plot of gravity yield parameter (Y_G) vs. yields Reynolds number (Re_τ) that shows the four general regions of behavior. In this plot, one can determine if a cavern exists in slurry or if solids will settle. The vertical line, $Y_G = 0.06$, is based on experimental results (Chhabra 1993)[13]. The horizontal line distinguishing between a cavern being present at low Re_τ and the jet causing fluid motion throughout the vessel needs to be determined either by an experiment or theory. In this study, we used the visual observations of the experiments, described below, and determined that cavern formation occurs at Yield Reynolds Numbers less than 30,000.

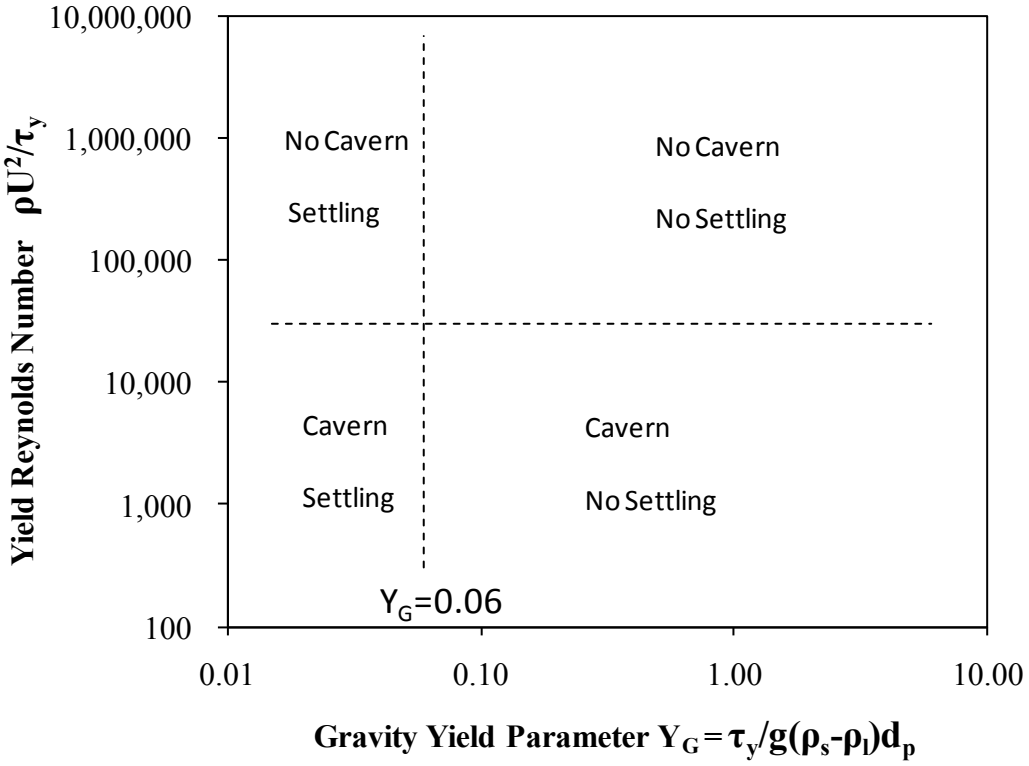

Figure 30: Regions of Behavior

The experimental visual observation is shown on the plot indicating that when YRe is less than 30,000 a cavern will exist. When Re_τ is increased above 30,000 the turbulent mixing and jet inertial will mobilize the vessel contents, and thus no cavern is formed. For particle settling (assuming a stagnant slurry), the SS seed particles will settle below Y_G of 0.06 and will not settle above this value. The preliminary results of this study were reported at the SSMD Sampling & Batch Transfer Results Workshop. [11]

Figure 31 compares the location of the various simulant tests with the full-scale mixing at three points. The full-scale MJPs have a jet velocity of 60 ft/s and the blue line shows the range of Re_τ and Y_G for the 100 micron seed particles at the full-scale velocity. The cohesive simulant testing conducted in this study spanned three different regions on this plot. The 0.3 Pa simulant (MJP operating 8 and 10 gpm) was in the region where there is no cavern (fluid motion occurred everywhere) and particles will settle within the carrier fluid. For these tests, the batch transfer and clearing radius behavior was equivalent to water. The 1.6 Pa simulant showed the beginning of cavern formation when the MJP was at 8 gpm, which is the slight lower positioned green datum. This test suggests the horizontal line should be at $Re_\tau \sim 30{,}000$. The 1.9 Pa simulant with the MJP at 10 gpm showed no cavern (fluid motion everywhere) and is appropriately above the horizontal line. These two tests are in a region where there is effectively no cavern and the seed particles should do not settle within the carrier fluid. For both of these tests, the batch transfer results showed more seed particles transferred in comparison to water but lower cleaning radius in comparison to the water tests. The 6.4 Pa simulant with the MJP at 10 gpm and 7.0 Pa simulant with the MJP at 8 gpm both showed a distinctive cavern and are appropriately below the horizontal line. During periods

of testing with these simulants, the MJP was operated at approximately 12 gpm to fully mix the tank. At 12 gpm, there was essentially no cavern (fluid motion everywhere) and again the horizontal line is appropriately located at 30,000. For these highest yield stress slurries, the region of behavior is to have a cavern and the seed particles should do not settle within the carrier fluid, and this is what was observed. For these tests, the batch transfer results showed even more seed particles transferred in comparison to water and even smaller cleaning radii.

The overall trend of increasing the slurry yield stress is a decrease in the observed cleaning radius but the total transfer of seed particles always increased with increasing yield stress. What appears to happen with jet mixing of yield stress slurries is that it is more difficult to suspend particles from the tank bottom with increasing yield stress, but the particles stay suspended to a greater degree once lifted from the tank bottom. The combine effect of increasing the yield stress is then an increase in the transfer of seed particles.

The full-scale tank operates at a higher jet velocity, and hence higher jet Reynolds number, and is shown with the blue line above the current test data. The current small-scale test conditions shown in Figure 31 indicate that the small-scale tests reported here include the key regions of full-scale behavior. A number of simple thought evaluations can be made with the current test data in comparison to the behavior that will occur at full-scale velocity. The green arrows show two extrapolations of the current test data to values of Re_τ and Y_G that represent full-scale jet velocity. For the green test data, moving to larger Re_τ should improve the cleaning radius and the overall mixing and suspension of particles. Moving to larger Y_G (for example smaller particles) should have less particle settling and hence better overall mixing and suspension. Both of these simple extrapolations suggest that the mixing behavior at full-scale will be improved. Similar arguments apply to the low- and high-yield stress data pairs. Overall, the current results for batch transfer showing the impact of cohesive particle interactions, which are reflected in a range of yield stress values, are expected to be representative of the impact of cohesive interactions in full-scale tank mixing.

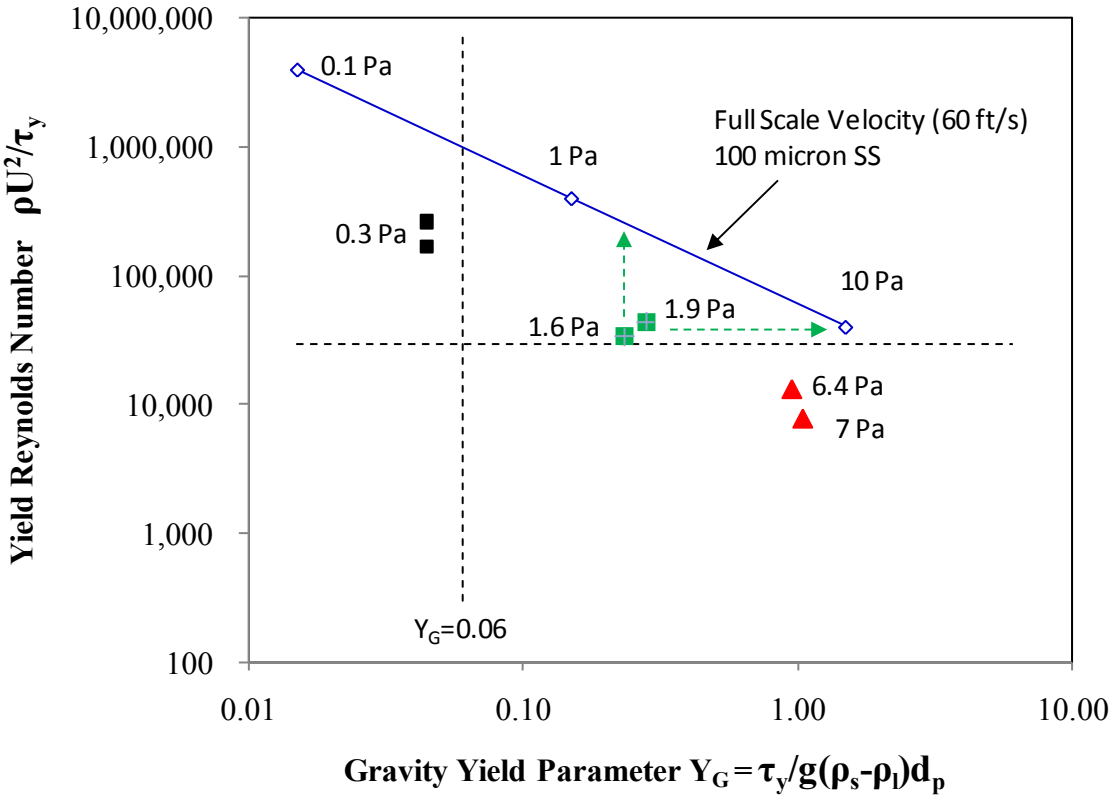

Figure 31: Gravity Yield vs. Yield Reynolds Number

The dimensional analysis indicates that the regions of behavior for full-scale mixing have been adequately represented by the current mixing/transfer demonstrations. Also, this analysis highlights the role of a yield stress (due to cohesive particle interactions) for the four regions of behavior and indicates how the results obtained in this study can be applied to the full-scale mixing behavior of DST waste. It should be noted that the location of the horizontal line for Re_τ was determined by the test data for the kaolin slurries and actual waste behavior may be somewhat different. Similarly, the location of the vertical line for Y_G was taken from the literature and actual waste behavior may again be somewhat different.

Figure 32 is a plot of the gravity yield number versus the average SS transferred to the Receipt Tanks. Only the tests with a simulant that had a yield stress and the water/SS test (Test 1) is included in the plot. The plot suggests as the Y_G for a simulant increases, the average transfer of solids also increased.

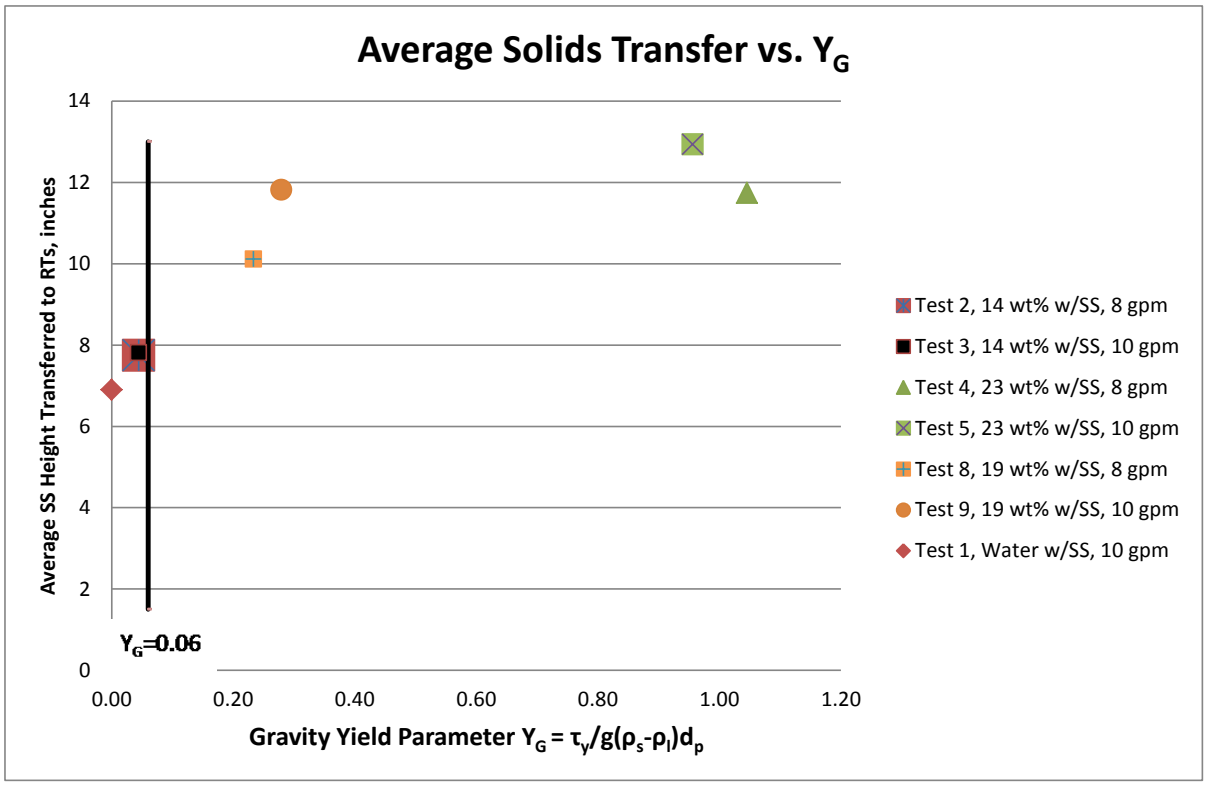

Figure 32: Gravity Yield vs. Average SS transferred to Receipt Tanks

4.0 CONCLUSIONS

- Testing results show that water always transfers less seed particles, and is conservative by this metric, when compared to fluids with a higher yield stress and/or higher viscosity at the same mixing/transfer parameters.

- A dimensional analysis highlighting the role of a yield stress (due to cohesive particle interactions) defined four regions of behavior and indicates how the results obtained in this study can be applied to the full-scale mixing behavior of DST waste. The analysis indicates that the regions of behavior for full-scale mixing have been adequately represented by the current small-scale tests.

- A comparison of testing results with slurries with Bingham yield stresses of 1.6 Pa to 7 Pa to a Newtonian glycerol/water mixture with a viscosity approximately equal to the Bingham consistency (viscosity) of the slurry shows very similar cleaning radius results, but the slurries had significantly increased batch transfer of seed particles. This finding shows that cohesive particle interactions, which impart a yield stress to the slurry, result in an overall increase in seed particle suspension and transfer, which is an improvement in mixing performance by this metric.

- Increasing the slurry yield stress decreased the observed cleaning radius but the total transfer of seed particles always increased with increasing yield stress. What appears to happen with jet mixing of yield stress slurries is that it is more difficult to suspend particles from the tank bottom with increasing yield stress, but the particles stay suspended to a greater degree once lifted from the tank bottom. The combined effect of increasing the yield stress is an increase in the transfer of seed particles.

- While mixing in the MDT, large SS particles settled from the simulant with no yield stress immediately after MJP jet passed.

- Large SS particles remained entrained (little to no settling) in simulant with a high yield stress. When the slurry set in the RTs overnight, there was visually no settling of SS.

- In comparison to water, more large, dense seed particles transferred from MDT to RTs in simulants with a yield stress ranging from 1.6 Pa to 7.0 Pa.

- The impact of non-Newtonian fluid properties depends on the magnitude of the yield stress. A higher yield stress in the carrier fluid resulted in more seed particles being transferred to the RTs.

- A fixed jet has a larger cleaning radius than a rotating jet at the same MJP jet nozzle velocity.

- MJP cleaning radius is impacted by the rheology of the fluid. The higher the yield stress the smaller the cleaning radius.

- Batch transfers of the cohesive simulants to the Receipt Tanks during Phase III were not as consistent as seen in Phase II where a salt simulant was used.

- For a given simulant, 10.0 gpm (28 ft/s per nozzle, U_oD=0.63 ft^2/s) to each MJP resulted in a larger, or better by this metric, batch transfer of seed particles when compared to the transfer of seed particles at 8.0 gpm (22.4 ft/s per nozzle, U_oD=0.504 ft^2/s) to each MJP. Thus, the amount of seed particles transferred is a direct result of the tank mixing.

- The simulant with a viscosity of 6.2 cP (YS= 0) had a large amount of seed particles transferred, or better transfer by this metric, when compared to the transfer of seed particles with water (1 cP) at the same mixing/transfer parameters.

- As found in past demonstrations, the lower amount, or poor consistency, of the solids transferred in batch 6 was due to low liquid level in the MDT resulting in poor mixing.

- TSPP eliminated the yield stress of the kaolin slurries, allowing the SS to settle in the RTs and this allowed visual observation of the quantity of seed particles transferred in each batch.

5.0 REFERENCES

1 Adamson, DJ, ML Restivo, TJ Steeper, DA Greer, "Demonstration of Mixer Jet Pump Rotational Sensitivity on Mixing and Transfers of the AY-102 Tank", SRNL-STI-2010-00521, Savannah River National Laboratory, Aiken, South Carolina, 2010

2 Adamson, DJ, MR Poirier, TJ Steeper, "Demonstration of Simulated Waste Transfers From Tank AY-102 to the Hanford Waste Treatment Facility", SRNL-STI-2009-00717, Savannah River National Laboratory, Aiken, South Carolina, 2009

3 Adamson, DJ, SRNL, PA Gauglitz, PNNL, "White Paper on Evaluation of Cohesive Simulants for Phase III Demonstrations", SRNL-L3100-2010-00224, Savannah River National Laboratory, Aiken, South Carolina, 2010

4 Hall MN. "*ICD 19 - Interface Control Document for Waste Feed*", 24590-WTP-ICD-MG-01-019, Rev. 4, River Protection Project, Waste Treatment Plant, Richland Washington, 2008.

5 Adamson, DJ, MR Poirier, TJ Steeper, "Demonstration of Internal Structures Impacts on Double Shell Tank Mixing Effectiveness", SRNL-STI-2009-00326, Savannah River National Laboratory, Aiken, South Carolina, 2009

6 Gauglitz, PA, BE Wells, JA Bamberger, JA Fort, J Chun, and JJ Jenks. "The Role of Cohesive Particle Interactions on Solids Uniformity and Mobilization During Jet Mixing: Testing Recommendations", PNNL-19245, Pacific Northwest National Laboratory, Richland, Washington, 2010.

7 Bamberger JA, LM Liljegren, and PS Lowery. 1990. "Strategy Plan – A Methodology to Predict the Uniformity of Double-Shell Tank Waste Slurries Based on Mixing Pump Operation." PNNL-7665, Pacific Northwest National Laboratory, Richland Washington.

8 Meyer PA, JA Bamberger, CW Enderlin, JA Fort, BE Wells, SK Sundaram, PA Scott, MJ Minette, GL Smith, CA Burns, MS Greenwood, GP Morgen, EBK Baer, SF Snyder, M White, GF Piepel, BG Amidan, A Heredia-Langner, SA Bailey, JC Bower, KM Denslow, DE Eakin, MR Elmore, PA Gauglitz, AD Guzman, BK Hatchell, DF Hopkins, DE Hurley, MD Johnson, LJ Kirihara, BD Lawler, JS Loveland, OD Mullen, MS Pekour, TJ Peters, PJ Robinson, MS Russcher, S Sande, C Santoso, SV Shoemaker, SM Silva, DE Smith, YF Su, JJ Toth, JD Wiberg, XY Yu, and N Zuljevic. 2009. "Pulse Jet Mixing Tests With Noncohesive Solids." PNNL-18098 (WTP-RPT-182, Rev. 0), Pacific Northwest National Laboratory, Richland, Washington.

9 Bamberger JA, PA Meyer, JR Bontha, CW Enderlin, DA Wilson, AP Poloski, JA Fort, ST Yokuda, HD Smith, F Nigl, MA Friedrich, DE Kurath, GL Smith, JM Bates, and MA Gerber. 2005. "Technical Basis for Testing Scaled Pulse Jet Mixing Systems for Non-Newtonian Slurries." PNWD-3551 (WTP-RPT-113 Rev. 0), Battelle—Pacific Northwest Division, Richland, Washington.

10 Chhabra RP. 1993. Bubbles, Drops, and Particles in Non-Newtonian Fluids. CRC Press, Boca Raton, Florida.

11 "SSMD Sampling & Batch Transfer Results Workshop Meeting Minutes and Presentations", WRPS-1101874, March, 2011

12 Enderlin CW, G Terrones, CJ Bates, BK Hatchell, and B Adkins. 2003. *Recommendations for Advanced Design Mixer Pump Operation in Savannah River Site Tank 18F*. PNNL-14443, Pacific Northwest National Laboratory, Richland, Washington

6.0 APPENDICES

Appendix A. DRAWINGS

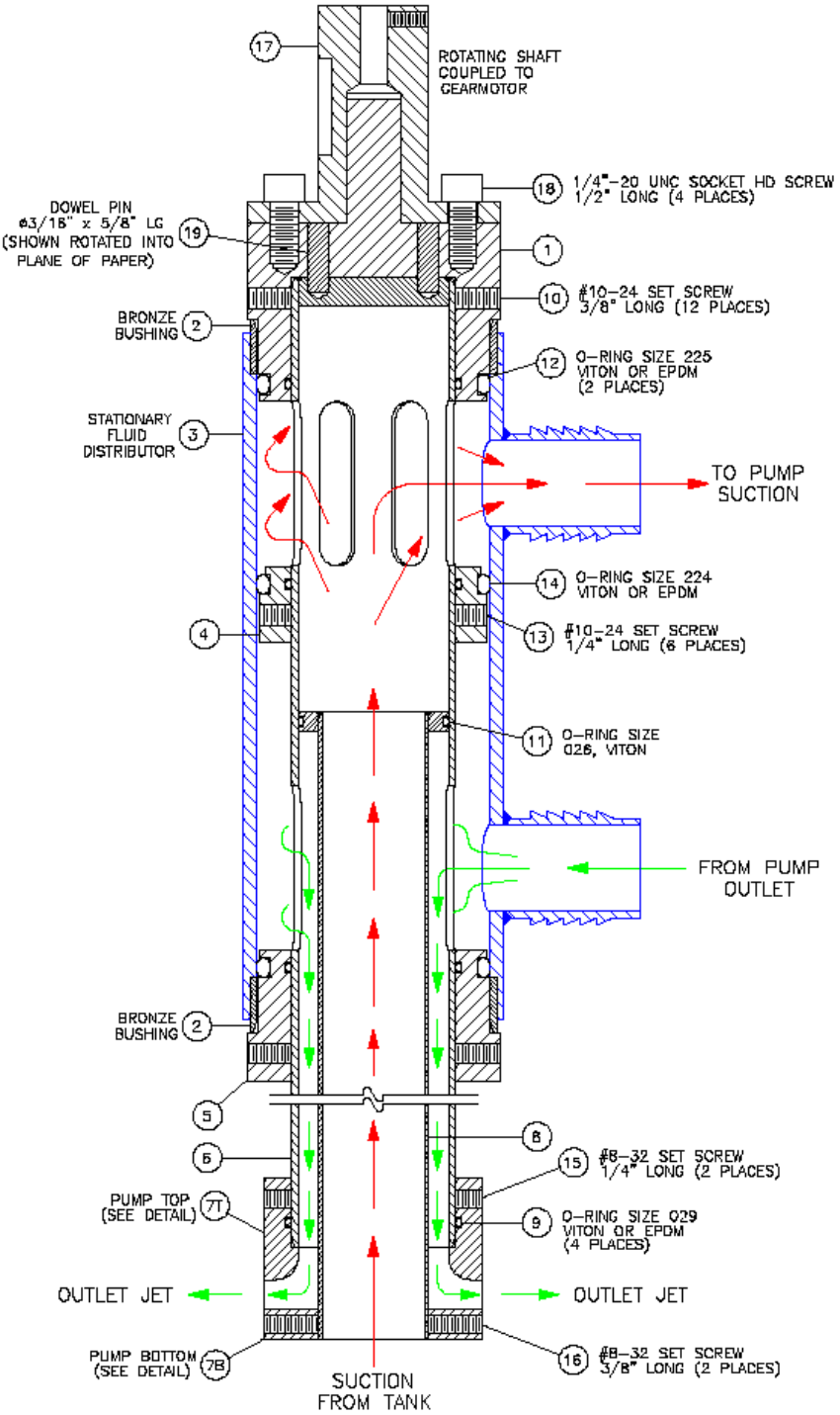

SCALED ROTATING MIXING PUMP
REVISED 05-17-2010

Figure A1: Mixer Jet Pump, Modified with bronze bushing & dowel pins

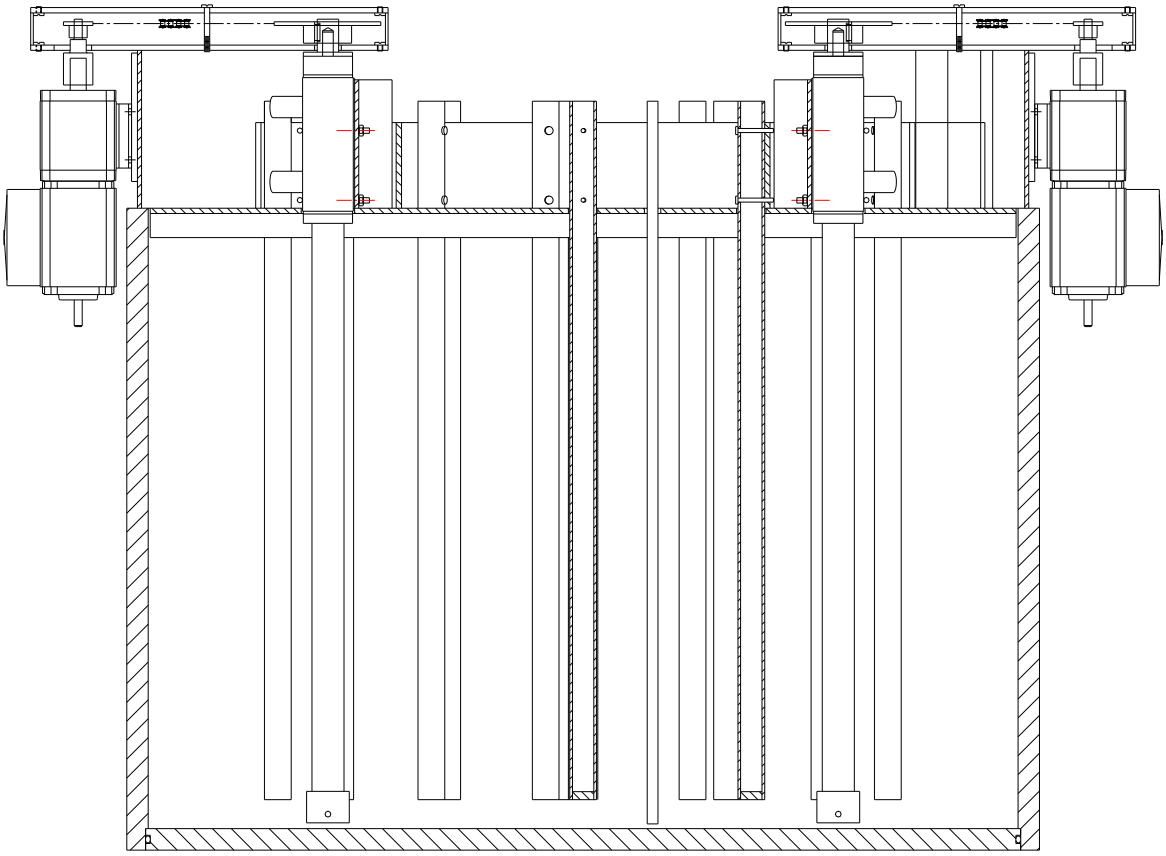

Figure A2: Side View of Obstructions MJP Assembly and Transfer Tubing

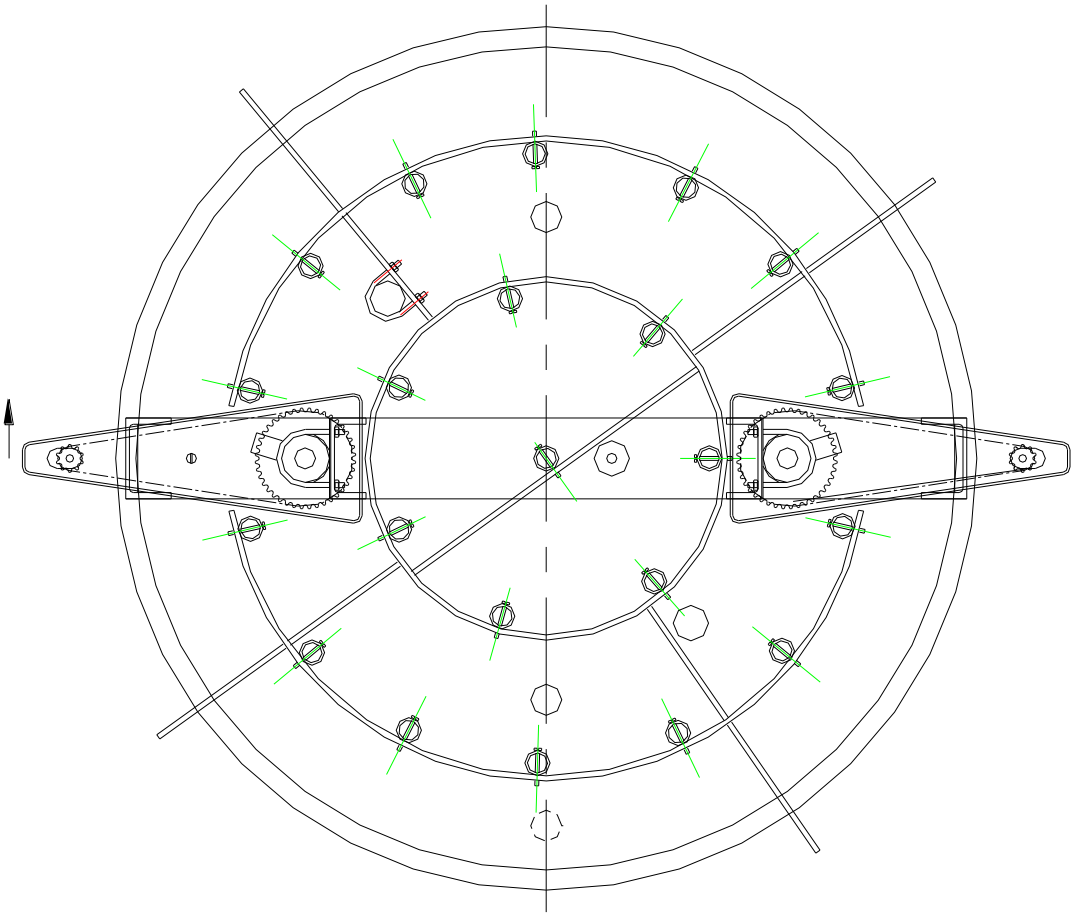

Figure A3: Top View of Obstructions and MJP Assembly

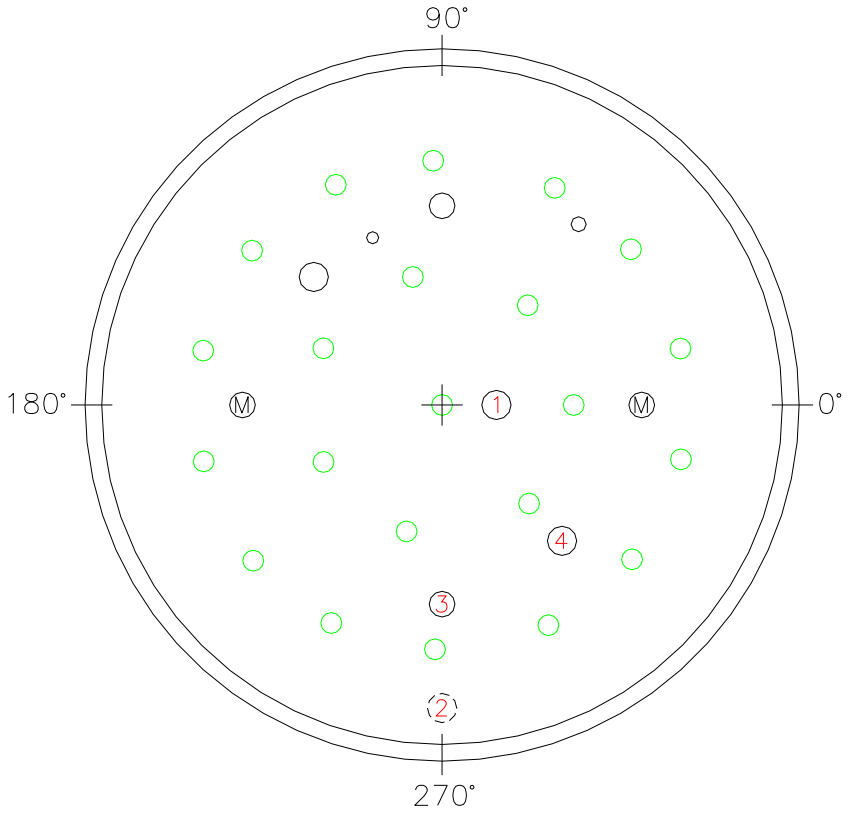

Figure A4: Top View of MDT (Transfer suction was only tested at Point 1, baseline)

Distribution:

A. B. Barnes, 999-W D. A. Crowley, 773-43A S. D. Fink, 773-A B. J. Giddings, 786-5A C. C. Herman, 999-W S. L. Marra, 773-A A. M. Murray, 773-A F. M. Pennebaker, 773-42A J. H. Scogin, 773-A W. R. Wilmarth, 773-A	